AWARD NUMBER: W81XWH-14-1-0171

TITLE: YY1 Control of AID-Dependent Lymphomagenesis

PRINCIPAL INVESTIGATOR: Michael Atchison

CONTRACTING ORGANIZATION: University of Pennsylvania
Philadelphia, PA 19104-6205

REPORT DATE: September 2016

TYPE OF REPORT: Final

PREPARED FOR: U.S. Army Medical Research and Materiel Command
Fort Detrick, Maryland 21702-5012

DISTRIBUTION STATEMENT: Approved for Public Release;
Distribution Unlimited

REPORT DOCUMENTATION PAGE

Form Approved
OMB No. 0704-0188

1. REPORT DATE	2. REPORT TYPE	3. DATES COVERED
September 2016	Final	July 1, 2014–June 30, 2016

4. TITLE AND SUBTITLE

YY1 Control of AID-Dependent Lymphomagenesis

5a. CONTRACT NUMBER

5b. GRANT NUMBER
W81XWH-14-01-0171

5c. PROGRAM ELEMENT NUMBER

6. AUTHOR(S)

Michael Atchison, PhD

E-Mail: atchison@vet.upenn.edu

5d. PROJECT NUMBER

5e. TASK NUMBER

5f. WORK UNIT NUMBER

7. PERFORMING ORGANIZATION NAME(S) AND ADDRESS(ES)

University of Pennsylvania
3451 Walnut Street, P221
Philadelphia, PA 19104-6205

8. PERFORMING ORGANIZATION REPORT NUMBER

9. SPONSORING / MONITORING AGENCY NAME(S) AND ADDRESS(ES)

U.S. Army Medical Research and Materiel Command
Fort Detrick, Maryland 21702-5012

10. SPONSOR/MONITOR'S ACRONYM(S)

11. SPONSOR/MONITOR'S REPORT NUMBER(S)

12. DISTRIBUTION / AVAILABILITY STATEMENT

Approved for Public Release; Distribution Unlimited

13. SUPPLEMENTARY NOTES

14. ABSTRACT

We hypothesized that YY1 levels control AID nuclear accumulation, AID mutation rates, and subsequent AID-mediated B cell lymphomagenesis. We tested this hypothesis by exploring the impact of YY1 overexpression, or deletion, in mouse lines that spontaneously develop AID-dependent B cell lymphoma. Our results suggest that overexpression of YY1 leads to higher mortality. To fully complete our analyses, these studies are on-going to include late time points in our studies. Second, we have bred the $yy1^{f/f}$ and γ1-CRE alleles onto the background of the mice that spontaneously develop AID-dependent B cell lymphoma. We found YY1 expression is critical for germinal center development and X-chromosome inactivation. Timed matings are ongoing to more fully establish the importance of YY1 loss in DLBCL at late time points. Finally, we have demonstrated that knock-out of YY1 results in reduced AID-mediated mutagenesis, supporting our main hypothesis. Four publications are expected. Two have been published, one is submitted, and an additional manuscript is in preparation.

15. SUBJECT TERMS

Nothing listed

16. SECURITY CLASSIFICATION OF:			17. LIMITATION OF ABSTRACT	18. NUMBER OF PAGES	19a. NAME OF RESPONSIBLE PERSON
a. REPORT	b. ABSTRACT	c. THIS PAGE			USAMRMC
Unclassified	Unclassified	Unclassified	Unclassified	35	19b. TELEPHONE NUMBER *(include area code)*

Table of Contents

Page

1. INTRODUCTION

Approximately 40% of all B cell lymphomas are derived from germinal center B cells and nearly half of patients with germinal center-derived diffuse large B cell lymphoma (DLBCL) are refractory to standard treatments, or undergo recurrences and have a very low chance of long-term survival. Activation induced cytidine deaminase (AID) is the mutagenic enzyme directly involved in germinal center B cell lymphomagenesis. Any factor that elevates nuclear AID levels will increase its mutagenic activity, thereby increasing the risk of lymphoma. Notably, we serendipitously found that transcription factor YY1 physically interacts with AID, promotes its stabilization, increases nuclear AID levels, and enhances AID function. Thus, our findings represent a new paradigm for control of AID function and B cell lymphomagenesis. We hypothesized that YY1 stabilization of nuclear AID directly contributes to B cell lymphomagenesis. We tested this hypothesis by modulating YY1 expression a mouse model, λmyc IμHABCL6, which spontaneously develops both AID-dependent and AID-independent B cell lymphomas. We tested our hypothesis in a powerful and innovative bone marrow transplantation model in which bone marrow from λmyc IμHABCL6 mice was transduced with YY1-expressing retrovirus or vector control, then injected into recipient mice to assess the ability of YY1 to impact development of B cell lymphoma. We also assessed the requirement for YY1 in lymphomagenesis by conditional deletion of the *yy1* gene in germinal center B cells using γ1-CRE mice. Our studies are still ongoing, but thus far support our model. YY1 may thus be a useful therapeutic target for DLBCL. In addition our studies showed that YY1 is crucial for germinal center B cell development, for X-chromosome inactivation in B lymphocytes, and for long distance DNA interactions in B cells.

2. KEYWORDS

Yin-Yang 1 (YY1), B Cell Lymphoma, Activation Induced Cytidine Deaminase (AID)

3. ACCOMPLISHMENTS

What were the major goals of the project?

Task 1. Does YY1 over-expression lead to increased lymphomagenesis or disease progression?

Our plan was to test our hypothesis that YY1 over-expression stabilizes nuclear AID, thereby promoting off target site mutations that drive B cell lymphomagenesis in a powerful and innovative bone marrow transplantation model in which bone marrow from λmyc IμHABCL6 mice is transduced with YY1-expressing retrovirus or vector control, and injected into secondary recipient mice.

1a. Isolate bone marrow from λmyc IμHABCL6 mice, transduce with YY1 retrovirus or vector control, inject into secondary recipient mice.

Time frame: months 1-12. 80% completed. Additional experiments are on-going.

1b. Evaluate tumor latency, tumor development by histology and pathology. Beginning 3 months after transduction and each month thereafter for 10 months, three mice from each group are sacrificed for evaluation of tumor development. Routine hematoxylin and eosin (H&E) stained slides of spleen, liver, lymph nodes, bone marrow, neoplastic tissue

and any other tissues that appear suspect are reviewed histologically by a board certified veterinary pathologist (Dr. Amy Durham). Germinal center phenotype is initially assessed by staining for PNA and CD95.
Time Frame: months 4-18. 40% completed. These experiments require long time-points, and the later time-point experiments are still on-going.

1c. Molecular profiling of tumors. Neoplasms isolated surgically are evaluated molecularly for mutations indicative of germinal center phenotype and by RNA microarray analyses for lymphoma subtyping. Mutations within Ig V and switch region DNA sequences are assayed by PCR amplification, cloning, and DNA sequencing. Mutations are also assessed within the BCL6, DC83, and Pim1 genes that are frequent targets of AID off-target mutations, with B2m, Ltb, Taci, Whsc1, H2Ea, A20 genes serving as negative controls. Translocations between c-myc and the IgH locus, or the miR-142 gene are measured by PCR followed by southern blotting. RNA prepared from tumors are subjected to microarray analyses using the Penn Vet microarray core facility. In particular we are assaying for transcript profiles consistent with a DLBCL phenotype (ABC and GC subtypes) and germinal center origin to determine if the observed tumors yield pre-germinal center, germinal center, or post-germinal center signatures as well as ABC and GC phenotypes.
Time Frame: months 6 to 24. 20% completed. These experiments require long time-points, and the later time-point experiments are still on-going. We anticipate completion in the coming year.

1d. Evaluation of tumor aggressiveness. Proliferation potential is assessed by growing splenic tumor cells ex vivo in the presence of LPS and measuring proliferation using CSFE staining. Tumor cells injected into sublethally irradiated (3 Gy) Rag -/- mice and time to tumor development and lethality are measured. Proliferation is measured by injecting BrdU into mice, isolating spleens, and staining with anti-BrdU, as well as the proliferation marker Ki-67. Apoptosis is assessed by TUNEL staining.
Time Frame: months 6 to 24. 20% completed. Tumor cells isolated in later time points still need to be collected. These studies will be completed in the coming year.

Task 2. Is YY1 necessary for B cell lymphomagenesis or disease progression?
We assessed the requirement for YY1 in lymphomagenesis using an innovative model in which YY1 expression is conditionally deleted from germinal center B cells of λmyc IμHABCL6 mice bearing a floxed YY1 locus by crossing with γ1-CRE mice. Development of B cell lymphoma in YY1-conditional null λmyc IμHABCL6 mice is assessed along with survival, tumor growth, and tumor sub-types as above. We predicted reduced B cell lymphomagenesis, extended latency time, and increased survival in the absence of YY1.
2a. Breed λmyc IμHABCL6 mice onto a $yy1^{f/f}$ γ-CRE background.
Time Frame: months 4-18. 100% completed

2b. Evaluate tumor latency, tumor development by histology and pathology. Beginning 3 months after birth and each month thereafter for 10 months, three mice are sacrificed each month for evaluation of tumor development. Routine hematoxylin and eosin (H&E)

stained slides of spleen, liver, lymph nodes, bone marrow, neoplastic tissue and any other tissues that appear suspect is reviewed histologically by a board certified veterinary pathologist (Dr. Amy Durham). Germinal center phenotype is initially assessed by staining for PNA and CD95
Time Frame: months 8-24. 50% completed. The mice are generated and later time points are still on-going. This will be completed in the coming year.

2c. Molecular profiling of tumors. Neoplasms are isolated surgically and evaluated molecularly for mutations indicative of germinal center phenotype and by RNA microarray analyses for lymphoma subtyping as described above in 1b.
Time Frame: months 8 to 24. 30% completed. The mice are generated and later time points are still on-going. This will be completed in the coming year.

2d. Evaluation of tumor aggressiveness. Proliferation potential and tumor aggressiveness will be assessed as described above in 1d.
Time Frame: months 6 to 24. 20% completed. Tumor cells isolated in later time points still need to be collected. These studies will be completed in the coming year.

What was accomplished under these goals?
Our major objective is to determine if YY1 levels impact the level of AID-dependent B cell lymphoma in mice. Specifically, we planned to either over-express YY1 in mice that spontaneously develop B cell lymphoma to determine if YY1 over-expression leads to increased lymphoma, or delete YY1 in the same mice to determine if this results in a reduction in B cell lymphoma.

Our significant results during the past year are below:
1. In task 1 we bred λmyc, IμHABCL6, and λmyc IμHABCL6 mice to generate sufficiently large colonies for our experiments. The mice bred somewhat slowly at first, which initially hampered progress, but these difficulties have been solved. Bone marrow from λmyc IμHABCL6 mice was transduced with retrovirus vectors consisting of either vector alone (MigR1) or YY1-expressing vector (MigR1-YY1). Transduced cells were transferred to secondary irradiated recipient mice and allowed to develop. In our preliminary experiments we found that the YY1-expressing mice became sick earlier than the MigR1-expressing mice. However, our numbers of analyzed mice were too low to be confident of this conclusion. We had higher than the normal level of death post-transplantation into irradiated recipient mice. We reduced this loss by giving the recipient mice water containing antibiotics two weeks prior to transplant rather than just coincident with transplant. The lower number of surviving mice than expected also initially hampered our ability to perform histology and to molecularly profile the tumors that develop. There was also a pinworm outbreak that resulted in a three month quarantine making it impossible to perform bone marrow transplants during that time period. All these complications have been solved and thus far our data supports a role for YY1 in DLBCL. As the experiments require long times of observation for tumor development, these experiments are on-going. We will complete these experiments in the

coming year despite the end date of this grant. Future publications will cite this grant support. We anticipate being able to fully accomplish this aim this year.

2. In task 2 we successfully bred the IμHABCL6 background into a $yy1^{f/f}$ γ-CRE background. This important step took many generations of breeding. These mice enable us to determine whether deletion of the *yy1* gene results in reduced B cell lymphoma. Such results would be very exciting and would indicate that YY1 should be explored as a potential target for treatment of B cell lymphoma. Our early time point experiments have been promising and suggest YY1 is important for DLBCL. To be certain of these results, later time points need to be evaluated. These experiments require timed mating to produced the affected and control mice, and these mice must be aged for many months to determine the impact of loss of YY1 on tumor development. These experiments are continuing past the end of this grant and future publications will cite this support. However, while these mice are aging, we were able to use this system to determine very exciting roles of YY1 in AID-mediated mutation, and in germinal center biology (sections 3 to 6, below).

3. In parallel experiments we obtained direct evidence that YY1 controls the mutation rate of AID. We looked at AID mutation rates in vivo in two different systems. First, we deleted YY1 in splenic B cells from IgκAID mice that overexpress AID leading to high mutation rates at the Smu region (an AID target site). Deletion of YY1 led to a statistically significant drop in the AID mutation rate at the Smu region, but not at the Taci gene (a non-AID target site) in agreement with our hypothesis (Fig. 1A, below). In a second system, $yy1^{f/f}$ mice which have normal AID expression levels, we found that deletion of the *yy1* gene led to a dramatic loss of AID-dependent mutations (Fig. 1B). This confirms our results in IgκAID mice and extends them into a more physiological setting. These results give us a high degree of confidence that our main hypothesis is true. This work will be submitted for publication shortly.

.

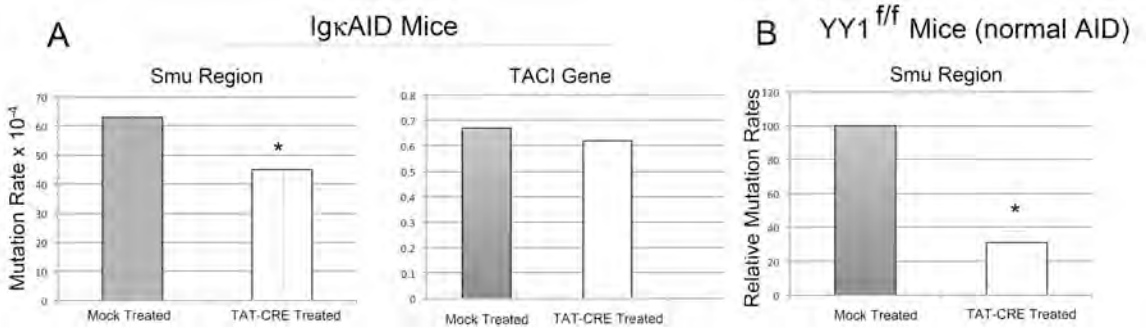

Figure 1. YY1 knock-out reduces AID mutagenic activity at AID-target sites. (A) Knock-out of YY1 reduces AID-mediated mutations at the AID-target Smu region, but not at the AID-nontarget TACI gene. (B) YY1 knock-out reduces AID mutation in mice with normal AID levels at the AID-target Smu region. Asterisks denote statistical significance $p<0.002$.

4. In the process of mating and expanding the mice for the experiments in task #2, we evaluated the importance of YY1 in germinal center development in $yy1^{f/f}$ γ1-CRE mice. These experiments showed that YY1 expression levels are highest in germinal center B cells. This is important because these are the cells that can give rise DLBCL. In addition,

knockout of YY1 resulted in a very dramatic absence of germinal center development and absence of germinal center B cells (Fig. 2). This work showed that YY1 is crucial for germinal center development and suggest that YY1 could be a valuable target for therapy against DLBCL. This work was published in PlosOne (see below, and Appendix).

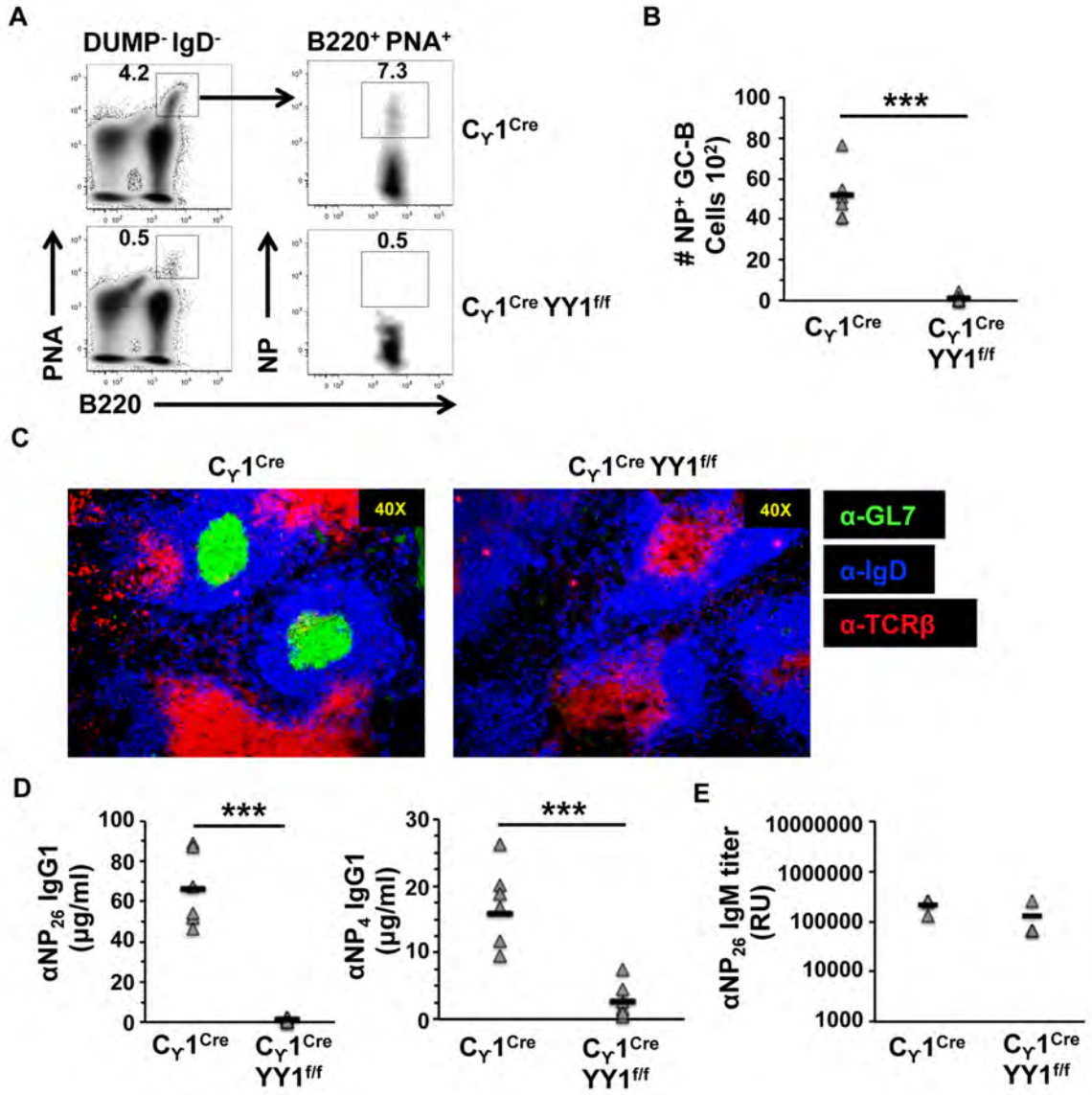

Figure 2. Antigen-specific GC cells are lost upon YY1 deletion. To determine the impact of YY1 conditional knock-out on germinal center B cells after initiation of an immune response, we injected mice with NP-chicken gamma globulin (NPP-CGG), a T cell-dependent antigen. After two weeks we collected blood and spleen to determine immune responses. Deletion of YY1 by γ1-CRE action in the yy1$^{f/f}$ γ1CRE line caused tremendous loss in the number of NP+ germinal center B cells compared to the γ1CRE line (Fig. 2A, B). This was confirmed by staining histological sections with fluorescent antibodies that recognize germinal center B cells (anti-GL7), follicular B cells (anti-IgD), and T cells (anti-TCRβ) (Fig. 2C), and by measuring serum IgG1 levels (Fig. 2D). Taken from our publication: Banerjee et al, 2016. (see below and Appendix)

5. In additional work we found that loss of YY1 may impact the development of autoimmune diseases. Females are more prone to autoimmune disorders, perhaps due to the X-chromosome, which contains many immunity-related genes. Female mammals use X-Chromosome Inactivation (XCI) to generate a transcriptionally silent inactive X chromosome (Xi) that is bound by Xist RNA, which equalizes gene expression between the sexes. We found mature naïve B cells have dispersed patterns of XIST/Xist RNA localization to the X chromosome but, i*n vitro* activation of B cells triggers the return of XIST/Xist RNA transcripts to the Xi in mouse and human lymphocytes. Remarkably, we found that conditional knock-out of YY1 ablates the ability of Xist RNA to bind to the inactive X-chromosome (Fig. 3). Thus, the Xi in female lymphocytes is predisposed to become partially reactivated and to overexpress immunity-related genes, providing the first mechanistic evidence for the enhanced immunity of females and their increased susceptibility for autoimmunity. This work was recently published in Proceeding of the National Academy of Science (see below; Appendix).

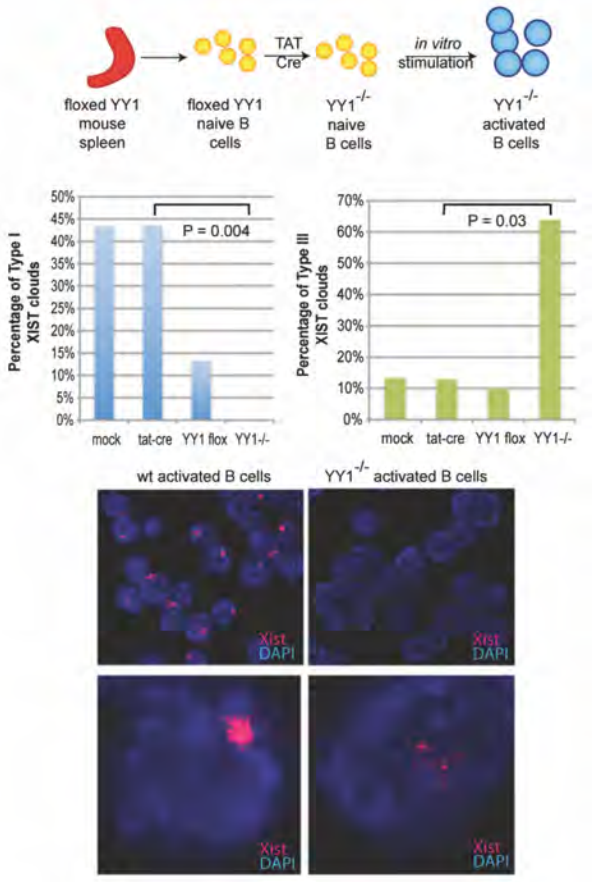

Figure 3. YY1 is needed for Xist localization to the inactive X chromosome. (Top) Experimental design for YY1 deletion in mouse B cells. (Middle) Quantification of Type I and Type III Xist RNA patterns in wildtype and YY1-/- activated B cells. Statistical significance calculated for averages from two independent experiments using Student's t test. (Bottom) Representative Xist RNA images for wildtype and YY1-/- activated B cells. Taken from Wang et al, 2016; see below, Appendix).

6. Activation of splenic B cells induces formation of a 220kb DNA loop between intronic and 3'RR enhancers in the immunoglobulin heavy chain locus (IgH). This DNA loop has been proposed to be necessary for the crucial immune diversification mechanism of IgH class switch recombination, but the factors that control its formation are unknown. We found that conditional deletion of transcription factor YY1 in primary splenic B cells results in a dramatic drop in formation of this DNA loop, as well as immunoglobulin class switch recombination. Reconstitution of YY1-deleted splenic B cells with various YY1 mutants showed that the C-terminal half of YY1 lacking the transactivation domain restored both intron-3'RR DNA loop formation as well as class switch recombination. RNA transcript analyses of YY1 conditional deleted splenic B cells suggested that YY1 does not regulate genes needed for DNA looping or CSR. Our results argue for a direct physical mechanism of YY1 mediating long-distance DNA loops and provide strong evidence of the importance of this DNA loop for class switching. Our results provide foundational mechanistic insight into a crucial immune function, and provide a possible additional mechanism for aberrant function leading to DLBCL, as defects in CSR can lead to chromosomal translocations and DLBCL as well as other lymphomas. This work has been submitted for publication.

What opportunities for training and professional development has the project provided?
Nothing to report.

How were the results disseminated to communities of interest?
Two publications thus far resulted from this work:

Banerjee, A., Sindhava, V., Vuyyuru, R., Jha, V., Hodewadekar, S., Manser, T., and Atchison, M.L. YY1 is required for germinal center development. PLoS ONE 2016 May 11;11(5):e0155311. doi: 10.1371/journal.pone.0155311. PMCID:PMC4833277

Wang, J., Syrett, C.M., Kramer, M.C., Basu, A., Atchison, M.L., Anguera, M.C. Unusual maintenance of X chromosome inactivation predisposes female lymphocytes for increased expression from the inactive X. Proc Natl Acad Sci U S A. 2016 Apr 5;113(14):E2029-38. doi: 10.1073/pnas.1520113113. PMCID: PMC4833277

What do you plan to do during the next reporting period to accomplish the goals?
This grant concluded on June 30, 2016, but we are actively continuing the work past this end date. Our plan for the coming year is largely to continue the work as outlined in Tasks 1 and 2. We will evaluate tumors resulting from transduced bone marrow with YY1 or vector expressing retroviruses, transplanted into irradiated recipient hosts, and will monitor tumor formation by histology and pathology, as well as by molecular profiling. Select samples will be evaluated for tumor aggressiveness.

Simultaneously we will evaluate the impact of YY1 knock-out on the latency, incidence, and aggressiveness of B cell lymphoma. Conditional YY1 knock-out mice will be evaluated for tumor development by histology and pathology, by molecular profiling, and by tumor aggressiveness.

We anticipate that our experiments will either support or disprove our hypothesis that YY1 expression levels regulate AID mutagenic activity, and as a consequence, the level of B cell lymphoma.

4. IMPACT

What was the impact on the development of the principle discipline of the project?

Our results have shown that reduction of YY1 levels impacts the rate of AID mutation in vivo. This is a very significant result and has a direct impact on the discipline of AID-mediated mutagenesis. We plan to finalize experiments to show this YY1-regulated change in AID mutation rates causes a corresponding change in the level and aggressiveness of AID-dependent B cell lymphomas. In addition, we made the seminal discovery that YY1 is critical for germinal center B cell development, and that YY1 can control function of the X-chromosome in B lymphocytes. Both of these discoveries emphasize the importance of YY1 for B cell development and its possible utility as a target for therapy against B cell malignancies. In work that has been submitted for publication, we found that YY1 is crucial for long distance DNA interactions needed for immunoglobulin class switch recombination. This seminal observation provides another mechanism by which YY1 may contributed to DLBCL (i.e., aberrant rearrangement of DNA).

What was the impact on other disciplines?

Our observations also directly impact other fields including immune functions and X-chromosome inactivation.

What was the impact on technology transfer?

Nothing to report.

What was the impact on society beyond science and technology?

Nothing to report.

5. CHANGES/PROBLEMS

Changes in approach and reasons for change

No significant changes in approach.

Actual or anticipated problems or delays and actions or plans to resolve them.

There were initial delays due to slow breeding by the mice. But this was resolved and the mice are breeding well now. We've also had higher than usual mortality of mice after bone marrow transplant. This problem was largely resolved and we anticipate no further delays in our work. Finally, a pinworm infection resulted in a 3 month quarantine which also hampered our work.

Changes that had a significant impact on expenditures

Nothing to report

Significant changes in use or care of human subjects, vertebrate animals, biohazards, and/or select agents.
Nothing to report

6. PRODUCTS

Publications, conference papers, and presentations
This work has already resulted in two excellent publications:

Banerjee, A., Sindhava, V., Vuyyuru, R., Jha, V., Hodewadekar, S., Manser, T., and Atchison, M.L. YY1 is required for germinal center development. PLoS ONE 2016 May 11;11(5):e0155311. doi: 10.1371/journal.pone.0155311. PMCID:PMC4833277

Wang, J., Syrett, C.M., Kramer, M.C., Basu, A., Atchison, M.L., Anguera, M.C. Unusual maintenance of X chromosome inactivation predisposes female lymphocytes for increased expression from the inactive X. Proc Natl Acad Sci U S A. 2016 Apr 5;113(14):E2029-38. doi: 10.1073/pnas.1520113113. PMCID: PMC4833277

One more manuscript is currently submitted. We anticipate that a fourth manuscript will be submitted for publication in the coming year.

Websites or other internet sites
Nothing to report

Technologies or techniques
Nothing to report

Inventions, patent applications, and/or licenses
Nothing to report

Other products
Nothing to report

7. PARTICIPANTS & OTHER COLLABORATING ORGANIZATIONS

What individuals worked on the project?

Name	Michael Atchison
Role on Project	PI
Nearest person month worked	2
Contribution to project	Overall supervision and direction
Funding support	NIH R01 AI079002, NIH GM111384, and Departmental sources

Name	Amy Durham
Role on Project	Pathologist
Nearest person month worked	2 total
Contribution to project	Pathology analyses
Funding support	Departmental sources

Name	Anupam Banerjee
Role on Project	Research Associate
Nearest person month worked	2
Contribution to project	Bone marrow transplants
Funding support	NIH R01 AI097590

Name	Parul Mehra
Role on Project	Research Associate
Nearest person month worked	4
Contribution to project	Generation of virus, bone marrow transplants, mouse breeding
Funding support	NIH R01 AI07002 and R01 GM111384

Name	Arindam Basu
Role on Project	Research Associate
Nearest person month worked	4
Contribution to project	Generation of virus, bone marrow transplants, isolation of cell populations
Funding support	NIH R01 AI07002 and R01 GM111384

Name	Aisha Ghias
Role on Project	Research Associate
Nearest person month worked	2
Contribution to project	General laboratory maintenance.
Funding support	NIH R01 AI07002 and R01 GM111384

Has there been a change in the active other support of the PD/PI or senior/key personnel since the last reporting period?
Nothing to report

What other organizations were involved as partners
Nothing to report

8. SPECIAL REPORTING REQUIREMENTS
Nothing to report

9. APPENDICES

Banerjee, A., Sindhava, V., Vuyyuru, R., Jha, V., Hodewadekar, S., Manser, T., and Atchison, M.L. YY1 is required for germinal center development. PLoS ONE 2016 May 11;11(5):e0155311. doi: 10.1371/journal.pone.0155311. PMCID:PMC4833277

Wang, J., Syrett, C.M., Kramer, M.C., Basu, A., Atchison, M.L., Anguera, M.C. Unusual maintenance of X chromosome inactivation predisposes female lymphocytes for increased expression from the inactive X. Proc Natl Acad Sci U S A. 2016 Apr 5;113(14):E2029-38. doi: 10.1073/pnas.1520113113. PMCID: PMC4833277

PLOS ONE

RESEARCH ARTICLE

YY1 Is Required for Germinal Center B Cell Development

Anupam Banerjee[1☯], Vishal Sindhava[1☯], Raja Vuyyuru[2¤], Vibha Jha[1], Suchita Hodewadekar[1], Tim Manser[2], Michael L. Atchison[1]*

1 Department of Biomedical Sciences, University of Pennsylvania, School of Veterinary Medicine, 3800 Spruce Street, Philadelphia, Pennsylvania 19104, United States of America, **2** Department of Microbiology and Immunology, Thomas Jefferson University, 233 South Tenth Street, Philadelphia, Pennsylvania 19107, United States of America

☯ These authors contributed equally to this work.
¤ Current address: Department of Immuno-Oncology, Bristol-Myers Squibb, Lawrenceville, New Jersey 08648 United States of America
* atchison@vet.upenn.edu

Citation: Banerjee A, Sindhava V, Vuyyuru R, Jha V, Hodewadekar S, Manser T, et al. (2016) YY1 Is Required for Germinal Center B Cell Development. PLoS ONE 11(5): e0155311. doi:10.1371/journal.pone.0155311

Editor: Yolande Richard, COCHIN INSTITUTE, Institut National de la Santé et de la Recherche Médicale, FRANCE

Received: February 3, 2016

Accepted: April 27, 2016

Published: May 11, 2016

Data Availability Statement: All relevant data are within the paper and its Supporting Information files.

Funding: This work was supported by R01 AI079002 http://www.niaid.nih.gov, R01 GM111384 http://www.nigms.nih.gov, and W81XWH-14-1-0171 http://mrmc.amedd.army.mil.

Competing Interests: The authors have declared that no competing interests exist.

Abstract

YY1 has been implicated as a master regulator of germinal center B cell development as YY1 binding sites are frequently present in promoters of germinal center-expressed genes. YY1 is known to be important for other stages of B cell development including the pro-B and pre-B cells stages. To determine if YY1 plays a critical role in germinal center development, we evaluated YY1 expression during B cell development, and used a YY1 conditional knock-out approach for deletion of YY1 in germinal center B cells (CRE driven by the immunoglobulin heavy chain γ1 switch region promoter; γ1-CRE). We found that YY1 is most highly expressed in germinal center B cells and is increased 3 fold in splenic B cells activated by treatment with anti-IgM and anti-CD40. In addition, deletion of the *yy1* gene by action of γ1-CRE recombinase resulted in significant loss of GC cells in both un-immunized and immunized contexts with corresponding loss of serum IgG1. Our results show a crucial role for YY1 in the germinal center reaction.

Introduction

Affinity maturation of immunoglobulins (Ig) in B cells largely occurs during the germinal center (GC) reaction where the processes of somatic hypermutation (SHM) and class switch recombination (CSR) occur [reviewed in references [1–3]]. B and T cells and that have been activated by antigen migrate to interfollicular regions in secondary lymphoid organs and interact [4,5]. These cells form long-lived interactions resulting in full B cell activation with increased expression of B Cell Lymphoma 6 (BCL6) protein and activation induced cytidine deaminase (AID) [6]. Activated cells migrate from the interfollicular region to the follicle where the B cells proliferate to begin formation of a germinal center [6,7]. Finally, the dark and light zones of the germinal center develop and B cells transition between these zones with SHM occurring in the dark zone, and affinity selection and CSR in the light zone. Ultimately the B

cells that are selected, mature into either memory B cells or plasma cells and exit the germinal center [1,2].

A number of transcription factors regulate the germinal center reaction. BCL6 is critical for germinal center formation as its deletion ablates GC formation [6,8]. A variety of other transcription factors effect either early or late germinal center formation and include Pax5, IRF4, IRF8, NF-κB, E2A, c-Myc, MEF2B, MEF2C, EBF1, and SpiB [1–3]. In addition, the histone methyltransferase EZH2 is crucial for GC formation [9]. These factors regulate gene expression profiles needed for germinal center formation and control cell proliferation which approaches the highest rates in mammalian systems [10].

Recently, transcription factor Yin Yang 1 (YY1) was proposed to be a master regulator of germinal center function [11]. Using computational approaches, Green and colleagues [11] characterized promoters of genes that are expressed in germinal center cells. The promoters of these GC signature genes were enriched in binding sites for YY1. In addition, it has been proposed that YY1 binding sites, as well as sites for E2A and C/EBPα are enriched within non-immunoglobulin regions of the genome where AID binds and generates off-target site mutations, perhaps involved in genesis of B cell malignancies [12]. Consistent with this idea, we showed that YY1 physically interacts with AID, leading to its stabilization and nuclear accumulation [13]. We also found YY1 conditional knock-out in splenic B cells, results in reduction of CSR [13]. Furthermore, YY1 is known to be critical for B cell development at other B cell stages. Using mb1-CRE, the Shi laboratory showed that conditional deletion of the *yy1* gene in early pro-B cells results in pro-B cell arrest, reduced IgH locus contraction, and reduced VDJ rearrangement of distal Vh genes [14]. Similarly we showed that deletion of the YY1 REPO domain needed for recruitment of Polycomb Group (PcG) proteins to DNA results in arrest at the pre-B cell stage and highly skewed Vκ gene rearrangement patterns [15]. We also showed that YY1 physically interacts with, and co-localizes with proteins involved in long-distance DNA contacts including condensin, cohesin, and PcG subunits [15]. Thus, YY1 clearly plays a significant role in B cell development.

Here we evaluated YY1 expression during B cell development, and used a γ1-CRE conditional knock-out approach to delete YY1 in germinal center B cells. We found that YY1 is most highly expressed GC B cells. Deletion of the *yy1* gene resulted in significant loss of GC cells in both un-immunized and immunized contexts. Our results show a crucial role for YY1 in the germinal center reaction.

Results

YY1 is highly expressed in germinal center B cells

As YY1 is a ubiquitously expressed transcription factor that has been proposed to be important for germinal center B cell development, we set out to determine relative YY1 protein levels at each stage of B cell development. For this we performed FACS with a fluorescent antibody against YY1 on various B cell populations from non-immunized mice. In bone marrow we gated on cell surface markers for pro-B ($B220^+$, $AA4.1^+$, $CD43^+$, $CD19^+$), pre-B ($B220^+$, $AA4.1^+$, $CD43^-$, $CD19^+$, $CD23^-$, IgM^-), immature B ($B220^+$, $AA4.1^+$, $CD43^-$, $CD19^+$, IgM^+), recirculating B ($B220^+$, $AA4.1^-$, $CD43^-$, $CD23^+$), and plasma cells ($DUMP^-$, IgD^-, $CD138^+$) (see strategy in Fig 1A and 1B). Staining intensity with anti-YY1 for each B cell fraction is shown in Fig 1C. From spleen we gated on markers for marginal zone ($B220^+$, $AA4.1^-$, $CD21/35^+$, $CD19^+$, $CD23^-$), follicular ($B220^+$, $AA4.1^-$, $CD23^+$, $CD19^+$, $CD21/35^+$), germinal center ($DUMP^-$, IgD^-, $GL7^+$, Fas^+), and plasma B cells ($DUMP^-$, IgD^-, $CDE138^+$) (see strategy in Fig 1D and 1E). Staining intensity with anti-YY1 for each B cell fraction is shown in Fig 1F. The

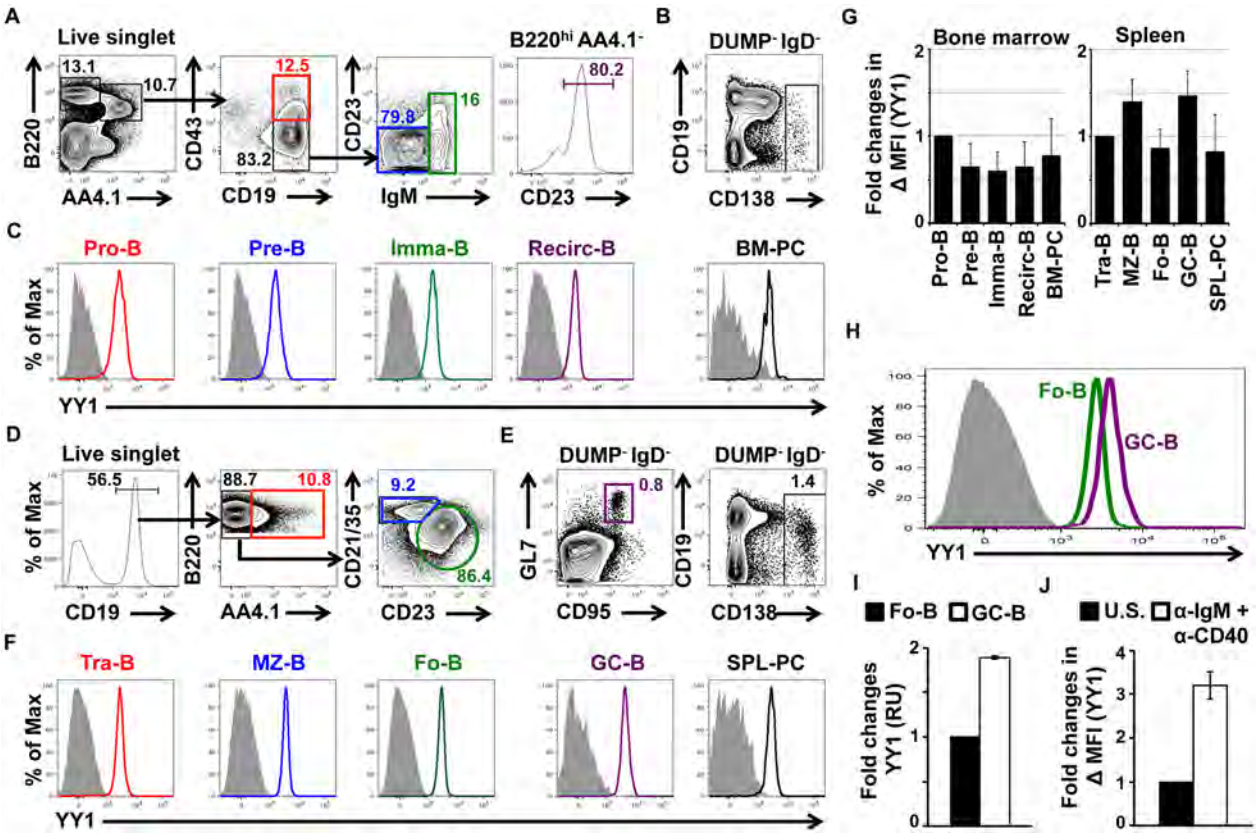

Fig 1. YY1 expression at various B cell developmental stages. (**A**) Bone marrow cells from non-immunized control $C\gamma1^{Cre}$ mice were stained with various antibodies to identify B cell developmental subsets, and **(B)** plasma cells. *A*. After doublet and dead cell discrimination, progenitor B cells (Pro-B) were phenotyped as $B220^{+}AA4.1^{+}CD19^{+}CD43^{+}$ cells; precursor B cells (Pre-B) were phenotyped as $B220^{+}AA4.1^{+}CD19^{+}CD43^{-}CD23^{-}IgM^{-}$ cells; immature B cells (Imma-B) were phenotyped as $B220^{+}AA4.1^{+}CD19^{+}CD43^{-}CD23^{+/-}IgM^{+}$ cells and recirculating mature B cells (Recirc-B) were phenotyped as $B220^{+}AA4.1^{-}CD23^{+}$ cells. *B*. We used CD138 to detect bone marrow plasma cells (BM-PC). We gated on $CD4^{-}CD8^{-}F4/80^{-}Gr1^{-}$(DUMP gate)$IgD^{-}$ cells that were $CD138^{+}$. **(C)** Bone marrow B cell subsets and plasma cells (gated as shown in A & B) were stained with anti-YY1 antibody or corresponding isotype control. (**D**) Spleen cells from Cγ1Cre mice were stained with various antibodies to identify B cell subsets (it should be noted that our follicular B cell gating may contain a very small percentage of B1 cells), **(E)** germinal center B cells (GC-B) and plasma cells (SPL-PC). *D*. After doublet and dead cell discrimination, transitional B cells (Tra-B) were phenotyped as $CD19^{+}AA4.1^{+}$ cells; marginal zone B cells (MZ-B) were phenotyped as $CD19^{+}AA4.1^{-}CD21/35^{hi}CD23^{lo}$ cells and follicular B cells (Fo-B) were phenotyped as $CD19^{+}AA4.1^{-}CD21/35^{lo}CD23^{hi}$ cells. *E*. GL7 and CD95 were used to detect GC-B cells, and CD138 to detect SPL-PC. We gated on $DUMP^{-}IgD^{-}$ cells that were further subdivided into $GL7^{hi}CD95^{hi}$ GC-B and $CD138^{+}$ SPL-PC. **(F)** Spleen B cell subsets, GC-B cells and SPL-PC (gated as shown in D & E) were stained with anti-YY1 antibody or corresponding isotype control. (**G**) Fold changes in mean fluorescence intensity (MFI) of YY1 in bone marrow B cell subsets (left panel, fold changes compared to pro-B cells) and spleen B cell subset (right panel, fold changes compared to tra-B cells). Fig A-G are representative results are from three independent experiments ($n = 3$ mice). **(H)** Comparison of YY1 staining of follicular and germinal center B cells. **(I)** Fo-B and GC-B cells were FACS sorted and YY1 expression was measured by qPCR. Expression was normalized to FO B cells ($n > 3$ mice). (J) Fold change in MFI of YY1 in un-stimulated (U.S.) or α-IgM + α-CD40 stimulated Fo-B cells after 3 days. Fig A-H are representative results from at least three independent experiments ($n = 3$ mice).

doi:10.1371/journal.pone.0155311.g001

comparative mean fluorescence intensity (MFI) in each B cell stage showed highest YY1 expression in germinal center B cells (Fig 1G and 1H).

By RT-PCR we found that YY1 transcripts were about 2 fold higher in germinal center B cells compared to follicular B cells (Fig 1I) corresponding with a roughly 2 fold increase in YY1 proteins levels as measured by MFI (Fig 1G and 1H). Activation of isolated splenic B cells with anti-IgM and anti-CD40 to mimic the germinal center activation phenotype caused a 3 fold increase in YY1 levels as measured by MFI (Fig 1J).

YY1 deletion by γ1-CRE activity impacts splenic B germinal center populations

To determine the importance of YY1 in germinal center development, we used the *yy1*$^{f/f}$ mouse line [14] that contains flox sites flanking the first exon in the *yy1* gene crossed with a *γ1CRE* line which expresses CRE recombinase from the IgH γ1 switch region promoter [16], to generate *yy1*$^{f/f}$ *γ1CRE* mice. The *γ1CRE* gene is expressed upon B cell activation initiating the germinal center reaction and this results in deletion of floxed genes within the first two days of the germinal center reaction [1].

Analyses of the naïve B cell populations present in spleen from non-immunized mice from each genotype (*yy1*$^{f/f}$, *γ1-CRE*, and *yy1*$^{f/f}$ *γ1-CRE*) showed that the transitional, marginal zone, follicular, and plasma B cell populations were relatively unchanged in each genotype (S1 Fig). Similarly, as expected, little differences were observed in bone marrow populations upon conditional deletion of YY1 by γ1CRE (S2 Fig). Thus, non-immunized *yy1*$^{f/f}$, *γ1CRE*, and *yy1*$^{f/f}$ *γ1CRE* mice showed the same levels of pro-B, pre-B, immature B, and recirculating B cells (S2 Fig). However, germinal center B cells showed a pronounced difference. Whereas *yy1*$^{f/f}$ and *γ1CRE* mice showed germinal center B cell populations of 0.9–0.8% of total cells, this population dropped nearly 10 fold to 0.097% in *yy1*$^{f/f}$ *γ1CRE* mice (Fig 2A). Whereas the percentage and number of total B cells remained unchanged, the percentage and number of germinal center B cells dropped dramatically in the *yy1*$^{f/f}$ *γ1CRE* line compared to *yy1*$^{f/f}$ and *γ1CRE* lines (Fig 2B and 2C). Thus, deletion of YY1 by action of the *γ1CRE* transgene resulted in loss in germinal center B cells. We observed no difference in the total number of T follicular helper (T_{FH}) cells in the yy1$^{f/f}$ γ1CRE mice compared to yy1$^{f/f}$ and γ1CRE mice, which are essential for germinal center formation and maintenance (S3A and S3B Fig). In addition, we did not observe any difference in follicular B cell proliferation in response to various stimuli suggesting no adverse impact of CRE expression on follicular B cells in yy1$^{f/f}$ γ1CRE mice (S3C Fig). Together, our results indicate that deletion of YY1 by action of the γ1CRE transgene resulted in loss of germinal center B cells.

We also measured serum Ig isotype levels in each genotype. As YY1 impacts germinal center B cell development where Ig CSR generally occurs, we anticipated that levels of IgM would remain similar, but that IgG1 isotype would be reduced in the *yy1*$^{f/f}$ *γ1CRE* background due to activation of the γ1-CRE gene. As expected, we found that IgM levels were comparable amongst the unimmunized *yy1*$^{f/f}$, *γ1CRE*, and *yy1*$^{f/f}$ *γ1CRE* lineages as were IgA, IgG2, and IgG3 (Fig 2D). However, levels of IgG1, and total IgG were greatly reduced in the *yy1*$^{f/f}$ *γ1CRE* line compared to the *yy1*$^{f/f}$ and *γ1CRE* lines (Fig 2D).

Antigen-specific GC cells are lost upon YY1 deletion

To determine the impact of YY1 conditional knock-out on germinal center B cells after initiation of an immune response, we injected mice with NP-chicken gamma globulin (NPP-CGG), a T cell-dependent antigen. After two weeks we collected blood and spleen to determine immune responses. Deletion of YY1 by γ1-CRE action in the *yy1*$^{f/f}$ *γ1CRE* line caused tremendous loss in the number of NP+ germinal center B cells compared to the *γ1CRE* line (Fig 3A and 3B). This was confirmed by staining histological sections with fluorescent antibodies that recognize germinal center B cells (anti-GL7), follicular B cells (anti-IgD), and T cells (anti-TCRβ) (Fig 3C). Thus, deletion of YY1 by γ1CRE caused loss of germinal center B cells, but not follicular B cells or T cells (Fig 3B).

We also determined the impact of YY1 deletion on high affinity verses low affinity antibodies against NP-CGG using NP(CGG)4 reactivity as definition of high affinity and NP(CGG)26 as low affinity. Deletion of YY1 caused a drop in both high affinity and low affinity IgG1

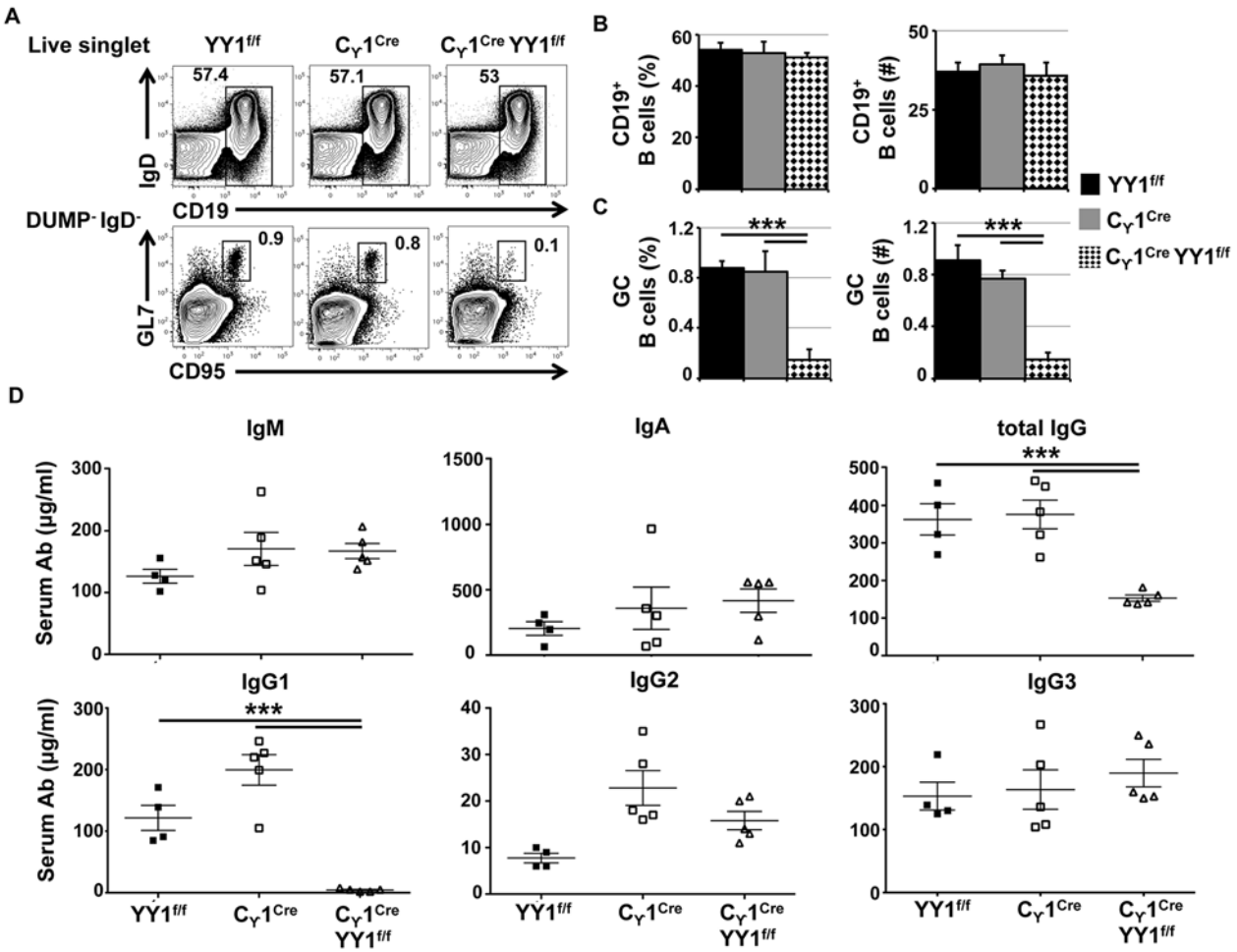

Fig 2. YY1 is required for germinal center B cell development and immunoglobulin class switching. (A) Spleen cells from non-immunized *YY1$^{f/}$*, *γ1CRE* and *YY1$^{f/f}$ γ1CRE* mice were stained with various antibodies to identify total B cells (CD19^{+}AA4.1^{+}, upper panel) and germinal center B cells (GC-B, DUMP^{-}IgD^{-}GL7^{hi}CD95^{hi}, lower panel). Percentages and number of **(B)** total B cells, and **(C)** GC-B cells per spleen of *YY1$^{f/}$*, *γ1CRE* and *YY1$^{f/f}$ γ1CRE* mice. Fig A-C are from three independent experiments (n = 3 mice for each genotype). **(D)** We used ELISA to detect various isotypes of serum immunoglobulins from *YY1$^{f/}$*, *γ1CRE* and *YY1$^{f/f}$ γ1CRE* mice. The concentration of IgM, IgA, total IgG, as well as IgG subclasses, IgG1, IgG2 and IgG3 were measured from sera samples that were obtained from four experiments ($n \geq 4$ mice for each genotype). Asterisks indicate p<0.001.

doi:10.1371/journal.pone.0155311.g002

antibodies against NP-CGG (Fig 3D). In contrast, IgM antibodies against NP-CGG produced by cells that have not entered the germinal center reaction were unaffected (Fig 3E). These results demonstrate that YY1 is critical for germinal center B cell development, germinal center-mediated immune responses, and loss of YY1 ablates the formation of germinal centers.

Discussion

Our results indicate that deletion of the *yy1* gene by action of γ1-driven CRE dramatically reduces the number of germinal center B cells in the spleen, as well as the histological appearance of germinal centers. The γ1 promoter is activated early in the germinal center reaction causing gene deletion within the first two days after antigen stimulation. This indicates that YY1 is critical for early events in germinal center development.

The phenotype with γ1CRE-mediated YY1 deletion is very similar to that observed upon EZH2 deletion using the same γ1CRE transgene [9]. EZH2 is a Polycomb Group (PcG) protein

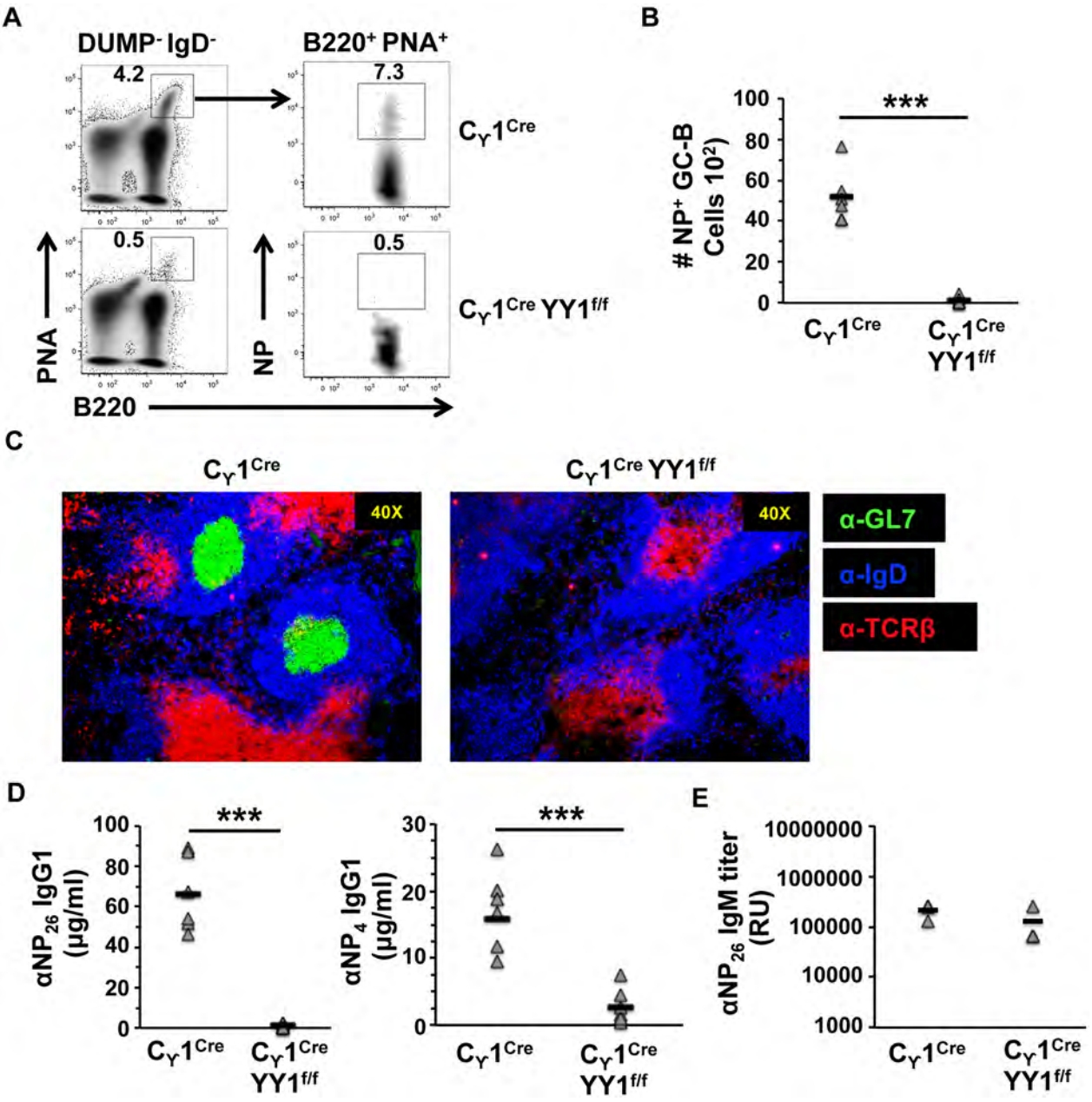

Fig 3. YY1 is required for antigen-specific germinal center development and for generation of antigen-specific IgG1. (A) Splenocytes from NP-CGG immunized *γ1CRE* and *YY1*$^{f/f}$ *γ1CRE* mice were harvested at 14 days after immunization and stained with various antibodies, as well as PNA to detect GC B cells. We gated on CD4$^-$CD8$^-$F4/80$^-$Gr1$^-$(DUMP$^-$) IgD$^-$ cells that were subdivided into PNA$^+$B220$^+$ GC-B cells. GC-B cells were gated and further subsetted into NP-specific (NP$^+$B220$^+$) GC-B cells. Representative results are from three independent experiments. **(B)** Numbers of NP-specific (NP$^+$B220$^+$) GC-B cells per spleen of immunized mice (n = 3). **(C)** *γ1CRE* and *YY1*$^{f/f}$ *γ1CRE* mice were immunized with NP-CGG, and 14 days later spleen sections were stained with anti-GL7, anti-IgD and anti-TCRβ antibody. GL7-rich regions demarcate germinal center B cells. **(D, E)** Serum from NP-CGG immunized *γ1CRE* and *YY1*$^{f/f}$ *γ1CRE* mice were collected at 14 days after immunization and NP-specific serum Igs were analyzed using ELISA. *D*. The concentration of low affinity (NP26, left panel) and high affinity (NP4, right panel) IgG1 in the serum. *E*. Titer of NP-specific total IgM in the sera of immunized mice. Data are derived from sera samples that were obtained from three experiments. Asterisks indicate p<0.001.

doi:10.1371/journal.pone.0155311.g003

component of the Polycomb Repressive Complex 2 (PRC2) and is responsible for trimethylation of histone H3 on lysine 27 leading to stable transcriptional repression [17–22]. EZH2 is also involved in cell proliferation and germinal center B cells are among the highest proliferating cells in mammalian systems [10]. EZH2 expression increases in germinal center B cells indicating its apparent importance in transcriptional repression or proliferation [23,24]. EZH2 is implicated in a number of malignancies and importantly, is directly involved in development of various lymphomas including diffuse large B cell lymphoma (DLBCL) derived from germinal center B cells [9,25,26].

Previously we showed that YY1 can function as a PcG protein to mediate PcG-dependent transcriptional repression [27]. Importantly, we found YY1 can recruit PcG proteins to specific DNA sequences to control histone H3 lysine 27 tri-methylation [28–31]. Interestingly, we previously showed that YY1 physically interacts with EZH2 [15], and can control its ability to bind to specific DNA sequences in in the genome [27–32]. However, it is unclear whether YY1 controls EZH2 DNA binding in germinal center B cells.

YY1 now joins a growing list of transcription factors involved in germinal center development including BCL6, IRF4, IRF8, NF-κB, E2A, c-Myc, MEF2B, MEF2C, EBF1, and SpiB [1–3]. Each factor appears to control various aspects of germinal center biology by either regulating germinal center-specific gene regulatory networks, or by controlling proliferation. Deletion of the *c-myc* gene by the same γ1-CRE gene used here also results in loss of germinal center B cells. c-Myc is needed for early germinal center formation as well as for germinal center maintenance [33,34]. It is believed that the importance of c-myc for germinal center formation and maintenance relates to its ability to control cell proliferation. Germinal center B cells proliferate at an extremely high rate and loss of this proliferation likely relates to loss of germinal center initiation as well as collapse of germinal center maintenance.

YY1 was proposed to regulate germinal center biology by regulating gene expression networks, as YY1 DNA binding sites lie within the promoters of genes expressed in germinal center B cells [11]. Consistent with this hypothesis, we found that YY1 protein is expressed at highest levels in germinal center B cells. However, YY1 controls multiple stages of B cell development. For instance, YY1 deletion early in B cell development by action of mb1-driven CRE results in arrest at the pro-B cell stage and loss of immunoglobulin heavy chain (IgH) locus contraction needed for distal Vh gene rearrangement [14]. In addition, the long distance DNA contacts needed for V(D)J rearrangement at the pro-B cell stage are ablated upon YY1 deletion [35,36]. At the pre-B cell stage, we showed that YY1 PcG function is required for generating complete Igκ gene repertoires, again likely due to impacting long-distance DNA loops needed for Vκ-Jκ rearrangement [15]. Finally, we showed that YY1 is important in mature splenic B cells for controlling IgH class switch recombination (CSR) [13]. While germinal center-specific genes may be regulated by YY1, the requirement for YY1 early in the germinal center reaction, and the ability of YY1 to control other stages of B cell development suggest that YY1 either impacts numerous distinct B cell stage-specific functions, or it controls common functions at each stage such as cell survival or proliferation. Indeed YY1 controls numerous housekeeping genes such as the ribosomal protein genes among others [37–39], and its complete knock-out results in early embryonic lethality [40]. Therefore, additional work will be necessary to determine the multiple and varied roles of YY1 in B cell development.

Materials and Methods

Mice and Immunization

We obtained *yy1*$^{f/f}$ mice from Dr. Yang Shi (Harvard University) and bred these mice with γ1-CRE mice generated by the Rawjewsky laboratory [16] and supplied by Jackson Laboratories

(Stock No: 010611). Work using mice followed recommendations in the Guide for the Care and Use of Laboratory Animals of the National Institutes of Health. The protocol was approved by the Institutional Animal Care and Use Committee of the University of Pennsylvania (Protocol 803080). Mice were immunized i.p. with 50μg NP-CGG in alum.

Flow Cytometry

For all analyses, bone marrow (BM) and spleens were disrupted to single cell suspension, and red blood cells were lysed using ACK buffer (Lonza). Equal numbers of cells were incubated with live/dead fixable aqua stain in PBS for 20 min at room temperature. Cells were washed and stained for surface antigens in PBS with 2% bovine serum albumin (BSA) for 30 min at 4°C. Following washing, cells were treated with Cytofix/Cytoperm buffer (eBiosciences) and then stained with antibodies against intracellular Ags for 30 min at 4°C. Data were collected on a BD LSR II flow cytometer and analyzed with FlowJo software (Tree Star). The antibodies used for flow cytometry were CD19 (clone 6D5), B220 (clone RA3-6B2), CD43 (clone S7), AA4.1/CD93 (clone AA4.1), CD23 (clone B3B4), CD21/35 (cloneBio4E3), IgD (clone 11–26), IgM (clone ll/41), CD4 (clone H129.19), CD8 (clone 53–6.7), F4/80 (clone BM8), Gr-1 (clone RB6-8C5), CD138 (clone 281–2), CD95/FAS (clone J02), GL7 (clone GL-7), CD62L (clone MEL-14), CXCR5 (clone RF8B2), FoxP3 (clone MF-14), PD-1 (clone J43), and YY1 (clone EPR4652). Exclusion of TOPRO-3 (Invitrogen) was used to identify live cells and doublets were excluded by forward and side scatter height versus width analysis.

ELISA

Ninety-six well plates were coated with 10μg/ml anti-Ig (H + L) (Southern Biotech) overnight at 4°C and blocked with PBS containing 2% BSA for one hour. Sera were incubated at various dilutions for one hour at room temperature. Detection was conducted using HRP-conjugated goat anti-mouse IgM, IgG, IgG1, $IgG2_{a+c}$, IgG3 or IgA (Southern Biotechnology) with a TMB substrate kit (BD Biosciences) and color development was quantified using EMax (Molecular Devices).

Immunohistochemistry

Spleens from NP-CGG immunized mice were collected on day 14 and immersed in O.C.T. (Tissue Tek), flash frozen using 2-methylbutane cooled with liquid nitrogen, and stored at −20°C. 8–10 μm sections were sliced in a cryostat, fixed with cold acetone, rehydrated in PBS, and incubated with antibodies in PBS containing 10% serum. Sections were stained with anti-GL7, anti-IgD and anti-TCRβ antibodies.

Supporting Information

S1 Fig. Flow scheme of B cell subsets and plasma cells in the spleen. (A) Spleen cells from *yy1*$^{f/f}$, *γ1CRE*, and *yy1*$^{f/f}$ *γ1CRE* mice were stained with various antibodies to identify B cell subsets, and **(B)** plasma cells (SPL-PC). *A*. After doublet and dead cell discrimination, transitional B cells (Tra-B) were phenotyped as $CD19^+$ $B220^+AA4.1^+$ cells; marginal zone B cells (MZ-B) were phenotyped as $CD19^+$ $B220^+AA4.1^-CD21/35^{hi}CD23^{lo}$ cells and follicular B cells (Fo-B) were phenotyped as $CD19^+$ $B220^+AA4.1^-CD21/35^{lo}CD23^{hi}$ cells. *B*. CD138 staining was used to detect SPL-PC. Splenocytes were gated on $DUMP^-IgD^-$ cells that were further subdivided into $CD138^+$ SPL-PC.
(TIF)

S2 Fig. Flow scheme of B cell subsets in the bone marrow. (A) Bone marrow cells from *yy1*$^{f/f}$, *γ1CRE*, and *yy1*$^{f/f}$ *γ1CRE* mice were stained with various antibodies to identify B cell developmental subsets, and re-circulating mature B cells. After doublet and dead cell discrimination, progenitor B cells (Pro-B) were phenotyped as B220^{+}AA4.1^{+}CD19^{+}CD43^{+} cells; precursor B cells (Pre-B) were phenotyped as B220^{+}AA4.1^{+}CD19^{+}CD43^{-}CD23^{-}IgM^{-} cells; immature B cells (Imma-B) were phenotyped as B220^{+}AA4.1^{+}CD19^{+}CD43^{-}CD23$^{+/-}$IgM^{+} cells and recirculating mature B cells (Recirc-B) were phenotyped as B220^{+}AA4.1^{-}CD23^{+} cells.
(TIF)

S3 Fig. Comparable T_{FH} cell numbers and Fo B cell proliferation in Cγ1Cre YY1$^{f/f}$ mice. (A) Representative staining of T_{FH} cells in YY1$^{f/f}$ mice. Live singlet cells were gated and subsetted into T_{FH} (CD4^{+}FoxP3^{-}CD62L^{-}PD1^{hi}CXCR5^{hi}) cells. **(B)** Number of T_{FH} cells per spleen of non-immunized YY1$^{f/f}$, Cγ1Cre and Cγ1Cre YY1$^{f/f}$ mice. Representative gating strategy to identify T_{FH} (CD4^{+}FoxP3^{-}CD62L^{-}PD1^{hi}CXCR5^{hi}) cells as shown in A (left). **(C)** MACS-sorted CD23^{+} Follicular B cells from YY1$^{f/f}$, Cγ1Cre and Cγ1Cre YY1$^{f/f}$ mice were labeled with CFSE and stimulated for 60 hours with anti-IgM (20 μg/ml), anti-IgM + anti-CD40 (2.5 μg/ml), LPS (5 μg/ml), or CpG (1 μM). At the end of the culture, live and dead cells were identified by TO-PRO-3 staining. CFSE dilution in the live cells is shown in the figure. Representative results are from three independent experiments.
(TIF)

Acknowledgments

We thank Yang Shi (Harvard) for providing *yy1*$^{f/f}$ mice and Michael Cancro (University of Pennsylvania) for helpful discussions.

Author Contributions

Conceived and designed the experiments: AB VS RV VJ SH TM MLA. Performed the experiments: AB VS RV VJ SH. Analyzed the data: AB VS RV VJ SH TM MLA. Contributed reagents/materials/analysis tools: TM MLA. Wrote the paper: AB VS RV SH TM MLA.

References

1. De Silva NS, Klein U (2015) Dynamics of B cells in germinal centres. Nat Rev Immunol 15: 137–148. doi: 10.1038/nri3804 PMID: 25656706
2. Basso K, Dalla-Favera R (2015) Germinal centres and B cell lymphomagenesis. Nat Rev Immunol 15: 172–184. doi: 10.1038/nri3814 PMID: 25712152
3. Recaldin T, Fear DJ (2015) Transcription factors regulating B cell fate in the germinal centre. Clin Exp Immunol 183: 65–75. doi: 10.1111/cei.12702 PMID: 26352785
4. Qi H, Cannons JL, Klauschen F, Schwartzberg PL, Germain RN (2008) SAP-controlled T-B cell interactions underlie germinal centre formation. Nature 455: 764–769. doi: 10.1038/nature07345 PMID: 18843362
5. Okada T, Miller MJ, Parker I, Krummel MF, Neighbors M, Hartley SB, et al. (2005) Antigen-engaged B cells undergo chemotaxis toward the T zone and form motile conjugates with helper T cells. PLoS Biol 3: e150. PMID: 15857154
6. Kitano M, Moriyama S, Ando Y, Hikida M, Mori Y, Kurosaki T, et al. (2011) Bcl6 protein expression shapes pre-germinal center B cell dynamics and follicular helper T cell heterogeneity. Immunity 34: 961–972. doi: 10.1016/j.immuni.2011.03.025 PMID: 21636294
7. Kerfoot SM, Yaari G, Patel JR, Johnson KL, Gonzalez DG, Kleinstein SH, et al. (2011) Germinal center B cell and T follicular helper cell development initiates in the interfollicular zone. Immunity 34: 947–960. doi: 10.1016/j.immuni.2011.03.024 PMID: 21636295
8. Dent AL, Shaffer AL, Yu X, Allman D, Staudt LM (1997) Control of inflammation, cytokine expression, and germinal center formation by BCL-6. Science 276: 589–592. PMID: 9110977

9. Béguelin W, Popovic R, Teater M, Jiang Y, Bunting KL, Rosen M, et al. (2013) EZH2 is required for germinal center formation and somatic EZH2 mutations promote lymphoid transformation. Cancer Cell 23: 677–692. doi: 10.1016/j.ccr.2013.04.011 PMID: 23680150

10. Allen CDC, Okada T, Cyster JG (2007) Germinal-center organizaton and cellular dynamics. Immunity 27: 190–202. PMID: 17723214

11. Green MR, Monti S, Dalla-Favera R, Pasqualucci L, Walsh NC, Schmidt-Supprian M, et al. (2011) Signatures of murine B-cell development implicate Yy1 as a regulator of the germinal center-specific program. Proc Natl Acad Sci U S A 108: 2873–2878. doi: 10.1073/pnas.1019537108 PMID: 21282644

12. Duke JL, Liu M, Yaari G, Khalil AM, Tomayko MM, Shlomchik MJ, et al. (2013) Multiple transcription factor binding sites predict AID targeting in non-Ig genes. J Immunol 190: 3878–3888. doi: 10.4049/jimmunol.1202547 PMID: 23514741

13. Zaprazna K, Atchison ML (2012) YY1 controls immunoglobulin class switch recombination and nuclear activation-induced deaminase levels. Mol Cell Biol 32: 1542–1554. doi: 10.1128/MCB.05989-11 PMID: 22290437

14. Liu H, Schmidt-Supprain M, Shi Y, Hobeika E, Barteneva N, Jumaa H, et al. (2007) Yin Yang 1 is a critical regulator of B-cell development. Genes Dev 21: 1179–1189. PMID: 17504937

15. Pan X, Papasani M, Hao Y, Calamito M, Wei F, Quinn WJ III, et al. (2013) YY1 controls Igκ repertoire and B-cell development, and localizes with condensin on the Igκ locus. EMBO J 32: 1168–1182. doi: 10.1038/emboj.2013.66 PMID: 23531880

16. Casola S, Cattoretti G, Uyttersprot N, Koralov SB, Seagal J, Hao Z, et al. (2006) Tracking germinal center B cells expressing germ-line immunoglobulin gamma1 transcripts by conditinoal gene targeting. Proc Natl Acad Sci U S A 103: 7396–7401. PMID: 16651521

17. Cao R, Wang L, Wang H, Xia L, Erdjument-Bromage H, Tempst P, et al. (2002) Role of histone H3 lysine 27 methylation in Polycomb-group silencing. Science 298: 1039–1043. PMID: 12351676

18. Simon JA, Kingston RE (2013) Occupying chromatin: Polycomb mechanisms for getting to genomic targets, stopping transcriptional traffic, and staying put. Molec Cell 49: 808–824. doi: 10.1016/j.molcel.2013.02.013 PMID: 23473600

19. Cao R, Zhang Y (2004) The functions of E(z)/EZH2-mediated methylation of lysine 27 in histone H3. Curr Opin Genet Dev 14: 155–164. PMID: 15196462

20. Lanzuolo C, Orlando V (2012) Memories from the Polycomb Group proteins. Ann Rev Genet 46: 561–589. doi: 10.1146/annurev-genet-110711-155603 PMID: 22994356

21. Kirmizis A, Bartley SM, Kuzmichev A, Margueron R, Reinberg D, Green R, et al. (2004) Silencing of human polycomb target genes is associated with methylation of histone H3 Lys 27. Genes Dev 18: 1592–1605. PMID: 15231737

22. Kuzmichev A, Nishioka K, Erdjument-Bromage H, Tempst P, Reinberg D (2002) Histone methyltransferase activity associated with a human multiprotein complex containing enhancer of Zeste protein. Genes Dev 16: 2893–2905. PMID: 12435631

23. Velichutina I, Shaknovich R, Geng H, Johnson NA, Gascoyne RD, Melnick AM, et al. (2010) EZH2-mediated epigenetic silencing in germinal center B cells contributes to proliferation and lymphomagenesis. Blood 116: 5247–5255. doi: 10.1182/blood-2010-04-280149 PMID: 20736451

24. Raaphorst FM, van Kemenade FJ, Fieret E, Hamer KM, Satijn DP, Otte AP, et al. (2000) Cutting edge: polycomb gene expression patterns reflect distinct B cell differentiation stages in human germinal centers. J Immunol 164: 1–4. PMID: 10604983

25. Caganova M, Carrisi C, Varano G, Mainoldi F, Zanardi F, Germain PL, et al. (2013) Germinal center dysregulation by histone methyltransferase EZH2 promotes lymphomagenesis. J Clin Invest 123: 5009–5022. doi: 10.1172/JCI70626 PMID: 24200695

26. van Kemenade FJ, Raaphorst FM, Blokzijl T, Fieret E, Hamer KM, Satijn DPE, et al. (2001) Coexpression of BMI-1 and EZH2 polycomb-group proteins associated with cycling cells and degree of malignancy in B-cell non-Hodgkin lymphoma. Blood 97: 3896–3901. PMID: 11389032

27. Atchison L, Ghias A, Wilkinson F, Bonini N, Atchison ML (2003) The YY1 transcription factor functions as a PcG protein in vivo. EMBO J 22: 1347–1358. PMID: 12628927

28. Srinivasan L, Atchison ML (2004) YY1 DNA Binding and PcG Recruitment Requires CtBP. Genes Dev 18: 2596–2601. PMID: 15520279

29. Wilkinson F, Pratt H, Atchison ML (2010) PcG recruitment by the YY1 REPO domain can be mediated by Yaf2. J Cell Biochem 109: 478–486. doi: 10.1002/jcb.22424 PMID: 19960508

30. Wilkinson FH, Park K, Atchison ML (2006) Polycomb recruitment to DNA in vivo by the YY1 REPO domain. Proc Natl Acad Sci USA 103: 19296–19301. PMID: 17158804

31. Basu A, Wilkinson FH, Colavita K, Fennelly C, Atchison ML (2014) YY1 DNA binding and interaction with YAF2 is essential for Polycomb recruitment. Nuc Acids Res 42: 2208–2223.

32. Srinivasan L, Pan X, Atchison ML (2005) Transient requirements of YY1 expression for PcG transcriptional rescue and phenotypic rescue. J Cell Biochem 96: 689–699. PMID: 16052488

33. Calado DP, Sasaki Y, Godinho SA, Pellerin A, Kochert K, Sleckman BP, et al. (2012) The cell-cycle regulator c-Myc is essential for the formation and maintenance of germinal centers. Nat Immunol 13: 1092–1100. doi: 10.1038/ni.2418 PMID: 23001146

34. Dominguez-Sola D, Victora GD, Ying CY, Phan RT, Saito M, Nussenzweig MC, et al. (2012) The proto-oncogene MYC is required for selection in the germinal center and cyclic reentry. Nat Immunol 13: 1083–1091. doi: 10.1038/ni.2428 PMID: 23001145

35. Guo C, Gerasimova T, Hao H, Ivanova I, Chakraborty T, Selimyan R, et al. (2011) Two forms of loops generate the chromatin conformation of the immunoglobulin heavy-chain gene locus. Cell 147: 332–343. doi: 10.1016/j.cell.2011.08.049 PMID: 21982154

36. Medvedovic J, Ebert A, Tagoh H, Tamir IM, Schwickert TA, Novatchkova M, et al. (2013) Flexible Long-Range Loops in the VH Gene Region of the Igh Locus Facilitate the Generation of a Diverse Antibody Repertoire. Immunity 39: 229–244. doi: 10.1016/j.immuni.2013.08.011 PMID: 23973221

37. Thomas MJ, Seto E (1999) Unlocking the mechanisms of transcription factor YY1: are chromatin modifying enzymes the key? Gene 236: 197–208. PMID: 10452940

38. Gordon S, Akopyan G, Garban H, Bonavida B (2006) Transcription factor YY1: structure, function, and therapeutic implications in cancer biology. Oncogene 25: 1125–1142. PMID: 16314846

39. Calame K, Atchison M (2007) YY1 helps bring loose ends together. Genes Dev 21: 1145–1152. PMID: 17504933

40. Donohoe ME, Zhang X, McGinnis L, Biggers J, Li E, Shi Y (1999) Targeted disruption of mouse Yin Yang 1 transcription factor results in peri-implantation lethality. Molec Cell Biol 19: 7237–7244. PMID: 10490658

Unusual maintenance of X chromosome inactivation predisposes female lymphocytes for increased expression from the inactive X

Jianle Wang[a], Camille M. Syrett[a], Marianne C. Kramer[b], Arindam Basu[a,1], Michael L. Atchison[a], and Montserrat C. Anguera[a,2]

[a]Department of Biomedical Sciences, School of Veterinary Medicine, University of Pennsylvania, Philadelphia, PA 19104; and [b]Department of Biochemistry and Biophysics, University of Pennsylvania Perelman School of Medicine, Philadelphia, PA 19104

Edited by Jeannie T. Lee, Harvard Medical School, Massachusetts General Hospital, Boston, MA, and approved February 23, 2016 (received for review October 11, 2015)

Females have a greater immunological advantage than men, yet they are more prone to autoimmune disorders. The basis for this sex bias lies in the X chromosome, which contains many immunity-related genes. Female mammals use X chromosome inactivation (XCI) to generate a transcriptionally silent inactive X chromosome (Xi) enriched with heterochromatic modifications and XIST/Xist RNA, which equalizes gene expression between the sexes. Here, we examine the maintenance of XCI in lymphocytes from females in mice and humans. Strikingly, we find that mature naïve T and B cells have dispersed patterns of XIST/Xist RNA, and they lack the typical heterochromatic modifications of the Xi. In vitro activation of lymphocytes triggers the return of XIST/Xist RNA transcripts and some chromatin marks (H3K27me3, ubiquitin-H2A) to the Xi. Single-cell RNA FISH analysis of female T cells revealed that the X-linked immunity genes *CD40LG* and *CXCR3* are biallelically expressed in some cells. Using knockout and knockdown approaches, we find that Xist RNA-binding proteins, YY1 and hnRNPU, are critical for recruitment of XIST/Xist RNA back to the Xi. Furthermore, we examined B cells from patients with systemic lupus erythematosus, an autoimmune disorder with a strong female bias, and observed different XIST RNA localization patterns, evidence of biallelic expression of immunity-related genes, and increased transcription of these genes. We propose that the Xi in female lymphocytes is predisposed to become partially reactivated and to overexpress immunity-related genes, providing the first mechanistic evidence to our knowledge for the enhanced immunity of females and their increased susceptibility for autoimmunity.

X chromosome inactivation | XIST RNA | epigenetics | female-biased autoimmunity

The X chromosome has the greatest density of immunity-related genes (1), and females, with two X chromosomes, have an immunological advantage over males (XY). Clinical studies have demonstrated that females have a more hyperresponsive immune system than males following immune challenges (2, 3). Females produce more serum IgM and antibodies (4, 5), which is immunologically advantageous, whereas males are more susceptible to bacterial and viral infections (5–7). This strong female-specific immune response is not always beneficial and can result in autoimmunity. Systemic lupus erythematosus (SLE) is an autoimmune disease where 85% of patients are women, yet the reason for this sex-based disparity is unknown (8, 9). The X chromosome is a critical factor for the breakdown of self-tolerance. Turner syndrome patients (XO) have a low risk of developing SLE (10), yet individuals suffering from Klinefelter's syndrome (XXY) have 14-fold increased risk of developing SLE (11), suggesting that gene dosage from the X chromosome somehow influences SLE susceptibility.

Females select one X for chromosome-wide transcriptional silencing in a process called X chromosome inactivation (XCI), which equalizes the expression of X-linked genes between genders (12, 13). XCI first takes place during embryonic development, where one X is chosen at random for silencing. This process is initiated by the allele-specific expression of the long noncoding RNA XIST in humans (14) and Xist in mice (15). After XCI initiation, the inactive X (Xi) enters the maintenance phase where XIST/Xist RNA remains associated with the Xi after each cell division (16). The Xi becomes enriched with additional heterochromatic modifications (H3K27me3, macroH2A, H3K9me2/3, H4K20me1, ubiquitin-H2A) and DNA hypermethylation (17–21), which promote gene repression (13). Female mammals silence most X-linked genes with XCI, yet some genes escape silencing (22). Approximately 15% of human X-linked genes are biallelically expressed in hybrid fibroblasts (23), whereas 3% of the mouse Xi escapes silencing (24). The expression level of escapee genes from the Xi is usually lower than from the active X (Xa). Escape from XCI can also vary between individuals (which enhances phenotypic differences), among cells within a tissue (25), and also during development and aging. The number of genes exhibiting variable escape from XCI is small: In humans, 10–12% display variable escape (23, 26), and in mice approximately 18 genes escape (24).

Because XCI is a mechanism to equalize gene expression between the sexes, there should be equal levels of immunity-related proteins in female and male cells. However, some immunity-related X-linked genes exhibit sex-biased expression, and this variability may predispose females toward developing

Significance

Females have increased immune responsiveness than males, and they are more likely to develop autoimmune disorders. The mechanism underlying these observations is unclear, and hypotheses suggest an important role for the X chromosome. Here, we discover that the inactive X is predisposed to become partially reactivated in mammalian female lymphocytes, resulting in the overexpression of immunity-related genes. We also demonstrate that lymphocytes from systemic lupus erythematosus patients have different epigenetic characteristics on the inactive X that compromises transcriptional silencing. These findings are the first to our knowledge to link the unusual maintenance of X chromosome Inactivation (the female-specific mechanism for dosage compensation) in lymphocytes to the female bias observed with enhanced immunity and autoimmunity susceptibility.

Author contributions: M.C.A. designed research; J.W., C.M.S., M.C.K., and A.B. performed research; M.L.A. contributed new reagents/analytic tools; J.W., C.M.S., and M.C.A. analyzed data; and M.C.A. wrote the paper.

The authors declare no conflict of interest.

This article is a PNAS Direct Submission.

[1]Present address: Pennsylvania State University, Brandywine Campus, Media, PA 19163.

[2]To whom correspondence should be addressed. Email: anguera@vet.upenn.edu.

This article contains supporting information online at www.pnas.org/lookup/suppl/doi:10.1073/pnas.1520113113/-/DCSupplemental.

autoimmunity (27). Altered expression of X-linked genes is observed in female-biased autoimmune disorders and mouse models of autoimmunity (8), raising the provocative notion that reactivation of genes from the Xi leads to the overexpression of immunity-associated X-linked genes that contribute to disease. Consistently, female, but not male, SLE patient $CD4^+$ T cells overexpress the X-linked genes *CD40LG* and *CXCR3* and their promoter regions are demethylated, suggesting that these genes are not overexpressed from the Xa, but are instead expressed from a reactivated Xi (28, 29). Because increased dosage of immunity-related genes such as *CD40LG* and *TLR7* are associated with SLE disease in human and mouse models, we investigated whether compromised maintenance of XCI in female lymphocytes from humans and mice could potentially contribute to predisposition toward autoimmunity. Notably, we demonstrate that fluctuations in the association of XIST/Xist RNA with the Xi may lead to partial reactivation, thereby increasing biallelic expression of autoimmune-associated genes.

Results

Female Lymphocytes Lack XIST RNA Transcripts on the Xi. To determine whether noncanonical XCI could potentially contribute to the increased risk of SLE in females, we examined the epigenetic characteristics of the Xi chromosome in human female mature lymphocytes. First, we performed RNA fluorescence in situ hybridization (FISH) by using two types of XIST-specific probes (double-stranded exon 1 region and short oligos). XIST/Xist RNA is expressed from the Xi in somatic cells, and the transcripts remain tightly associated, forming a cloud-like structure that is visualized by RNA FISH (16, 30). Remarkably, bulk T cells from human females did not have the canonical XIST RNA cloud observed in other somatic cells (Fig. 1*A*). This result was consistent, regardless of T-cell purification method [fluorescence activated cell sorting (FACS) or negative selection with magnetic beads] or collection procedure (apheresis or traditional venipuncture). The majority of FACS sorted naïve $CD4^+$ and $CD8^+$ T cells and female naïve B cells also lacked XIST RNA clouds, resembling male T cells (Fig. 1*B*). Similar results were obtained by using single-molecule oligo probes for XIST (Fig. S1*A*, *Left* and *B*, *Right*). Mature naïve splenic T cells from female mice also lacked Xist RNA clouds (Fig. 2*D*, *Top*), in contrast with a previous study where Xist RNA signals were detected in 25–60% of $CD4^+$ and $CD8^+$ T cells (31).

We observed that female naïve lymphocytes have four distinct patterns of XIST RNA localization: Type I nuclei contain tightly clustered pinpoints localized with one X, similar to those in female fibroblasts; type II nuclei have diffuse pinpoints of XIST RNA that roughly encompass a nuclear area the size of one X; type III nuclei have dispersed pinpoints extending beyond the X chromosome territory; and type IV nuclei lack XIST RNA signal (Fig. 1*C*). We quantified the number of cells with each class of XIST RNA localization pattern and found that naïve T cells are mostly type III,

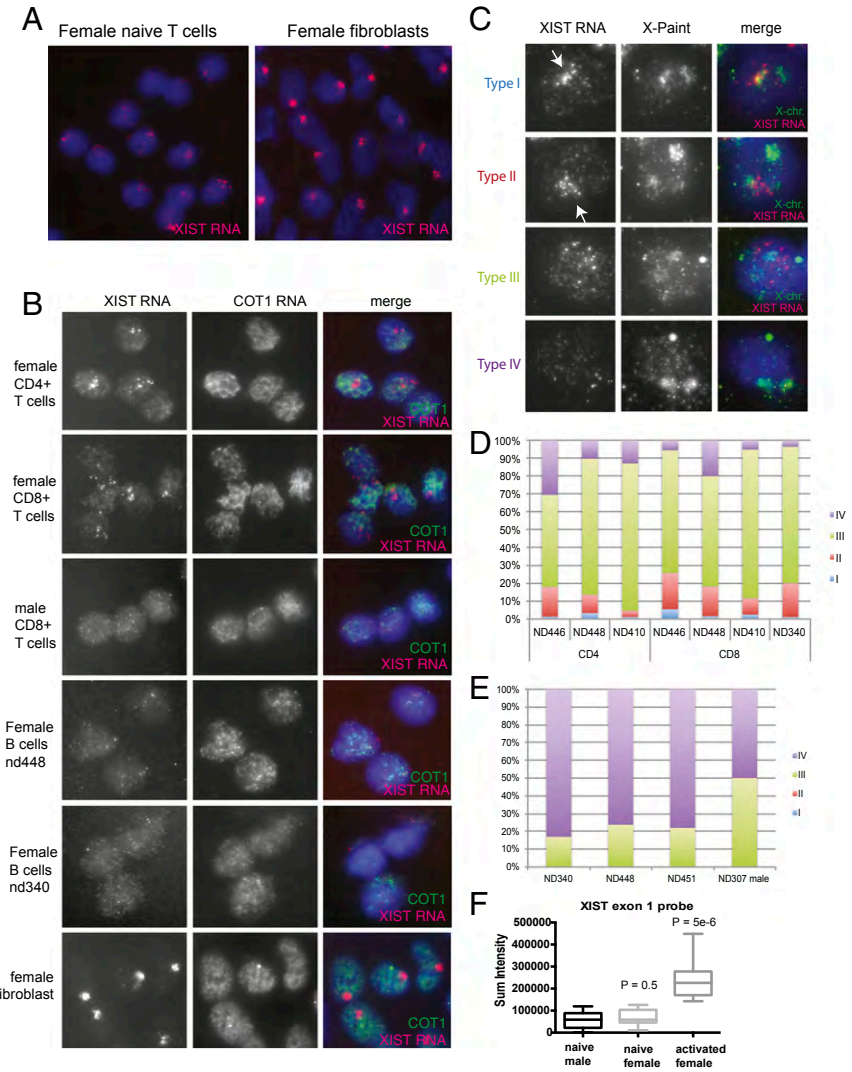

Fig. 1. Naïve human lymphocytes lack canonical XIST RNA clouds on the Xi. (*A*) RNA FISH analysis for XIST RNA and COT1 RNA, for naïve T cells and female fibroblast cell line (IMR-90). (*B*) XIST (red) and COT1 (green) RNA FISH for sorted mature naïve lymphocytes from human males and females. (*C*) Diversity of XIST RNA localization patterns (types I, II, III, IV) in naïve human lymphocytes. Sequential RNA FISH (for XIST RNA) followed by DNA FISH (to identify the two X chromosomes) at single-cell resolution. Arrows denote the inactive X chromosome. (*D*) Quantification of each type of XIST RNA localization pattern for naïve $CD4^+$ and $CD8^+$ T cells. (*E*) XIST RNA localization patterns for naïve B cells. (*F*) Quantification of total fluorescence for XIST RNA FISH using exon 1 probe for 12 nuclei for each cell type.

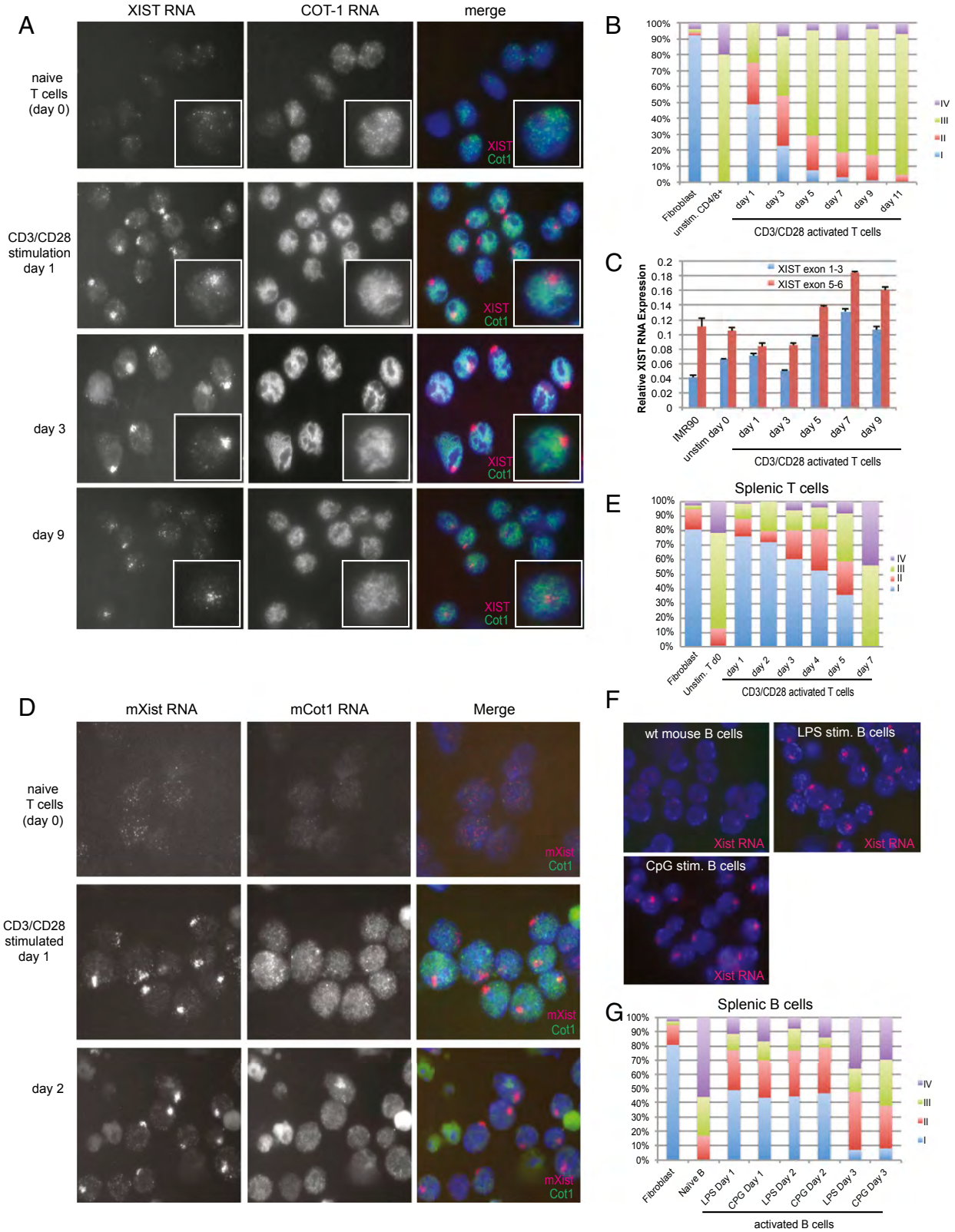

Fig. 2. XIST/Xist RNA transcripts return to the Xi in activated T and B cells. (*A*) Representative XIST and COT1 RNA FISH images of human naïve T cells stimulated in vitro. Stimulation of five different individuals yielded similar results. (*B*) Quantification of each class of XIST RNA localization pattern (types I–IV) after stimulation for cells from the same individual. (*C*) qRT-PCR for XIST RNA in naïve and activated T cells using primer sets for both the 5′ and 3′ ends. (*D*) Xist RNA and Cot1 RNA FISH analyses of mouse naïve T and in vitro activated T cells. (*E*) Xist RNA localization in activated mouse T cells. (*F*) Xist RNA FISH using female mouse mature naïve B cells and activated B cells stimulated in vitro using lipopolysaccharaide (LPS) or CpG DNA (CpG). (*G*) Xist RNA localization patterns for activated mouse B cells.

followed by type II and IV patterns (Fig. 1*D*). Roughly 1–4% of human female naïve T cells had type I XIST RNA clouds. Next, we repeated RNA FISH by using single-molecule oligo probes specific for human XIST and found that naïve female T cells had greater fluorescence sum intensities ($P = 0.05$) and maximum intensities ($P = 8.0e{-}6$) compared with male T cells (Fig. S1*B*). We also quantified the numbers of each type of XIST RNA localization pattern for human female naïve B cells and observed a different distribution of XIST RNA localization pattern relative to T cells, irrespective of the collection method. Mature naïve B cells contain mostly type III and IV nuclei, and we never detected a type I XIST RNA cloud (Fig. 1*E*). In summary, naïve T and B cells are the first female somatic cells to our knowledge where the Xi is missing clustered XIST RNA transcripts.

XIST/Xist RNA Returns to the Xi upon Lymphocyte Activation. Naïve lymphocytes are quiescent, and upon antigen recognition can become activated and reenter the cell cycle. We investigated the XIST RNA localization patterns in female T cells activated in vitro by using CD3/CD28 and performed a time course analysis of XIST RNA FISH following in vitro stimulation. We discovered that XIST RNA clouds return to the Xi 24 h after in vitro stimulation (Fig. 2*A*). The XIST clouds formed after 1–3 d of stimulation, and resembled clouds present in female fibroblasts (Fig. 1*A*), with the XIST RNA territory located in a COT-1 negative space within the nucleus (Fig. 2*A*). We observed similar RNA FISH results when using a double-stranded probe for *XIST* exon 1 or single-molecule oligo probes for XIST together with COT-1 (Fig. S1*A*). Activated female T cells exhibited greater nuclear fluorescence sum intensity and maximum intensity values compared with naïve female and male T cells, reflecting the presence of the XIST RNA transcript concentrated on the Xi (Fig. 1*F* and Fig. S1*B*). Because RNA FISH does not accurately reflect transcript absence, we used more sensitive quantification methods for XIST RNA (see below).

Because COT-1 RNA detects regions of nascent transcription within the nucleus (32–34), our observations of XIST clouds within COT-1 holes suggest that XIST localization promotes transcriptional silencing of the chromosome (Fig. 2*A*). Quiescent naïve T cells had a faint COT-1 signal, with speckled pinpoints distributed across the nucleus (Fig. 2*A*). Activated T cells had a greater overall COT-1 signal and defined nuclear distribution patterns for cells at days 1–3 following stimulation (Fig. 2*A*). Type I XIST RNA clouds decreased in activated T cells at day 5 following stimulation, with a concomitant increase in the number of cells with type III RNA pinpoints (Fig. S2 *A* and *B*). The percentages of type IV clouds, which lack XIST RNA signal, did not change after stimulation. In vitro stimulation resulted in a maximum of 30–50% of cells with type I XIST RNA clouds and 25–40% type II XIST pinpoints, and the distribution varied by individual (Fig. 2*B* and Fig. S2*A*). Type I cells disappeared by day 7, and COT-1 RNA patterns became diffuse by days 9–11 (Fig. S2*B*), consistent with increased apoptosis (visualized as nonspecific fluorescence and smaller DAPI nuclei).

We also examined mature naïve T and B cells isolated from female mouse spleens and found that, like human cells, these cells also lack canonical Xist RNA clouds (Fig. 2 *D* and *F*). Bulk female mouse T cells (typically 90% pure) contained similar amounts of helper T cells ($CD4^+$) and cytotoxic T cells ($CD8^+$), and roughly 10% of $CD4^+$ cells were regulatory T cells ($FoxP3^+$) (Fig. S2*C*). In vitro stimulation of mouse bulk T and B cells promoted the return of Xist RNA clouds to the Xi, with the greatest numbers of type I pattern observed 1 d after activation (Fig. 2 *E* and *G*). In vitro-activated mouse T cells had the most type I Xist RNA clouds (~75%), even higher than human T cells where a maximum of 50% of cells contained the canonical XIST RNA cloud. We verified T-cell activation efficiency by using FACS to sort $CD44^+$ cells (expressed on activated T cells) and the percentages of actively dividing cells using CFSE labeling (Fig. S2*D*). Type I Xist clouds persisted in activated mouse T cells for longer periods compared with activated human cells, yet by day 7, the cells reverted to type III and IV patterns and increased apoptotic cells (denoted by autofluorescence) (Fig. 2*E* and Fig. S3*A*). Next, we activated mature B cells in vitro two ways: either by adding lipopolysaccharide or CpG (35, 36). Type I Xist RNA clouds returned to the Xi following stimulation of B cells, similar to T-cell activation, irrespective of the method used for activation (Fig. 2 *F* and *G*). B cells stimulated for 1 d had the most type I Xist RNA clouds (45%), but never reached the levels in female mouse embryonic fibroblasts or T cells.

Because both human and mouse mature naïve T cells lack typical XIST/Xist RNA clouds, we investigated whether these cells express *XIST*/*Xist*. We used quantitative PCR (qPCR) to quantify the steady-state levels of human XIST RNA and mouse Xist RNA in naïve and activated lymphocytes. Remarkably, XIST/Xist RNA was abundant in naïve and activated T cells in human (Fig. 2*C* and Figs. S3*B* and S4*A*) and mouse (Fig. S4 *C* and *D*), and the levels were nearly equivalent to those found in female fibroblasts. We found that *XIST*/*Xist* was also highly expressed in naïve human (Fig. S4*A*) and mouse B cells (Fig. S4*B*), which had different XIST RNA localization patterns than naïve T cells. Because naïve T cells are quiescent and have reduced transcriptional activity, we repeated the quantitative RT-PCR (qRT-PCR) analyses normalizing for cell number. We also normalized XIST/Xist RNA expression by using a housekeeping gene (*RPL13A*), whose expression does not change with in vitro lymphocyte stimulation (37). We found that the levels of Xist RNA were similar for naïve and activated T cells, regardless of the method used for normalization (Fig. S4*D*). Similar to T cells, activated female mouse B cells also expressed equivalent levels of Xist RNA compared with naïve B cells (Fig. S4*B*). Northern blot analyses using equal amounts of RNA from mouse naïve and activated T cells support our qRT-PCR results that naïve female lymphocytes contain similar levels of Xist RNA transcripts as activated cells (Fig. S4*E*). We observed that Xist Northern blots of mouse T cells resembled Xist Northern blots of mouse embryonic stem cells and differentiating cells (38), with a multitude of high and low molecular weight bands of Xist transcripts. We found that female naïve T cells had a more intense signal of Xist RNA transcripts compared with activated T cells, but both samples had the same pattern of Xist RNA bands. We did not observe significant RNA degradation between naïve and activated female T-cell samples (Fig. S4*E*). Our results are in agreement with previous findings that XIST/Xist RNA transcription and transcript localization are independent processes (39, 40). We conclude that mammalian female naïve and activated lymphocytes have similar levels of XIST/Xist RNA transcripts to produce the canonical type I cloud, yet naïve lymphocytes are unable to properly localize these transcripts to the Xi.

The Chromatin of the Xi Is More Euchromatic in Mammalian Lymphocytes. Quiescent lymphocytes, which have a reduced transcriptional program, contain regions of facultative chromatin that become decondensed following activation (41). The mammalian Xi is enriched for histone H3K27me3, histone H2A ubiquitin (H2AUb), histone H4K20me1/3, histone H3K9me3, and the histone variant macroH2A (17, 20, 42–44). These marks form a focus that colocalizes with the Xi (and the XIST/Xist RNA cloud) when visualized cytologically in sequential RNA FISH and immunofluorescence (IF) experiments. Because naïve lymphocytes are quiescent and contain more heterochromatin than activated cells (45), they should theoretically exhibit enriched heterochromatic modifications on the Xi. However, because XIST RNA does not localize to the Xi in naïve lymphocytes, these modifications might also be missing. Therefore, we examined the localization of H2AUb, H3K27me3, macroH2A, or H4K20me1 with the Xi in mature naïve lymphocytes by using RNA FISH for detection of XIST/Xist RNA followed by IF for each modification, and finally DNA FISH to identify the two X chromosomes. Female fibroblasts were used as a positive control, and foci were observed overlapping XIST/Xist RNA signal for human and mouse cells. In human naïve T cells, we did not detect nuclear foci

for H2AUb, H3K27me3, macroH2A, or H4K20me1 modifications that colocalized with an X chromosome (Fig. 3*A*). Mouse naïve T cells also lacked foci of H2AUb, H3K27me3, H3K9me3, and macroH2A that colocalized to the Xi (Fig. 3*B*). This observation is in agreement with a previous study showing that macroH2A is never detected over the Xi in female mouse mature lymphocytes (41). Although we detected abundant nuclear signal for all of these repressive modifications in both human and mouse T cells, we never observed a focus that overlapped with an X chromosome. We conclude that the mammalian Xi lacks enrichment of heterochromatic modifications in mature naïve lymphocytes.

We repeated the serial RNA FISH/IF/DNA FISH analyses by using in vitro activated bulk T cells, and observed that some, but not all, heterochromatin marks returned to the Xi. Specifically, we found that H2AUb and H3K27me3 modifications formed foci in 70–80% of nuclei, and that these foci overlapped the type I XIST/Xist RNA cloud (Fig. 3 *A* and *B*). Remarkably, the return of these heterochromatic modifications to the Xi occurred in both human and mouse T cells. MacroH2A staining intensity was high throughout the nucleus of activated mouse and human T cells, yet focal enrichment on the Xi was observed for only 12–15% of nuclei with type I XIST/Xist patterns (Fig. 3 *A* and *B*). In activated human T cells, we observed the most pronounced macroH2A foci in type II nuclei with diffuse XIST RNA pinpoints (Fig. 3*A*). H4K20me1/3 modifications returned to the Xi in roughly 50% of human T cells (Fig. 3*A*). We conclude that the chromatin of the Xi in female T cells is different compared with fibroblasts, and that mature naïve cells have a more euchromatic Xi because it is missing H3K27me3, H4K20me, macroH2A, and H2AUb enrichment.

Female Lymphocytes Exhibit Partial X-Reactivation Resulting in Increased Expression of Immunity-Related X-Linked Genes. We examined how this unusual chromatin affects expression of two X-linked genes, *CD40LG* and *CXCR3*, frequently overexpressed in the autoimmune disorder SLE. Our hypothesis was that the euchromatic features of the Xi would result in expression of genes from the Xi in naïve and stimulated human T cells. We used sequential RNA then DNA FISH to detect expression of three X-linked genes subject to XCI (*CD40LG, CXCR3*, and *ATRX*). To identify the location of the Xi, we used a probe for XIST RNA to identify the Xi (for RNA FISH). Lastly, we denatured the slides for DNA FISH, which detected the location of the two X chromosomes. We quantified the percentages of cells expressing these genes from just the Xa or both Xs by counting the number of cells containing one pinpoint (monoallelic) or two pinpoints (biallelic) that overlapped with

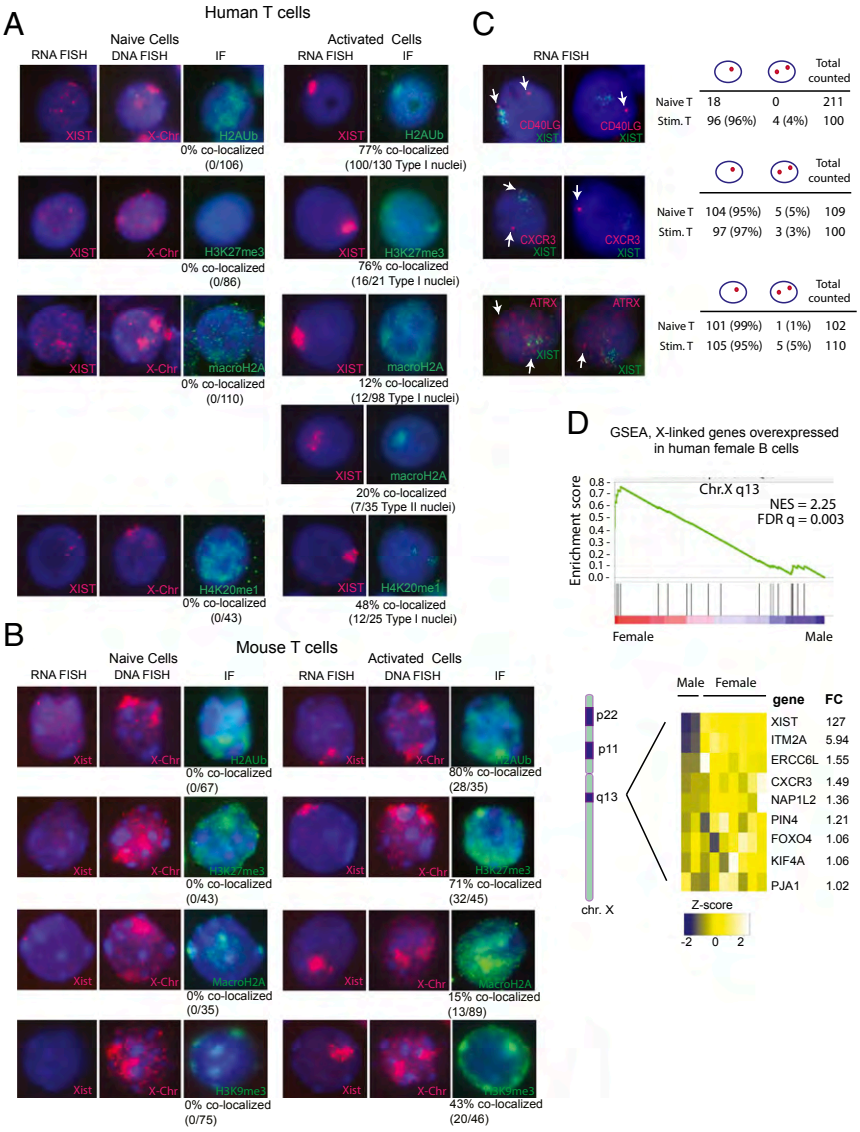

Fig. 3. The Xi has euchromatic features in mammalian lymphocytes. Sequential XIST RNA FISH, then immunofluorescence detection (and X-Paint to detect both X chromosomes) for naïve and activated T cells from humans (*A*) and mice (*B*). (*C*) Allele-specific expression (using RNA FISH) of *CD40LG, CXCR3,* and *ATRX* in activated human female T cells at single-cell resolution. White arrows indicate nascent transcripts from each X. (*D*) GSEA analysis comparing global gene expression differences with human female (seven samples) to male naïve B cells (two samples). Chromosome X map shows three regions on the X that have higher expression in female B cells. Heatmap lists the overexpressed genes in female naïve B cells from region chrX.q13 and fold-change (FC) values.

an X chromosome. We examined mature naïve and in vitro stimulated T cells from healthy human female and male donors, which are a positive control for monoallelic expression. We found that human naïve T cells had dimmer (but still detectable) RNA FISH signals compared with day 3 stimulated cells (Fig. S5). Analysis of *CD40LG,* an X-linked gene overexpressed in $CD4^+$ T cells from female SLE patients (23, 26, 28), revealed the presence of mostly monoallelic (96% with one pinpoint) and some biallelic expression (4% with two pinpoints), in activated female T cells (Fig. 3*C*). We were unable to detect a clear *CD40LG* nascent transcription signal in naïve female T cells, despite repeated efforts with cells from different female donors. Male T cells were exclusively monoallelic for *CD40LG* expression (Fig. S5*A*), as expected. Next, we repeated the analysis by using a probe specific for *CXRC3*, another X-linked gene subject to XCI that is frequently overexpressed in female SLE $CD4^+$ T cells (23, 26, 28). Again, we detected some naïve (5%) and stimulated T cells (3%) with biallelic expression of *CXCR3* (Fig. 3*C* and Fig. S5*B*). As a control, we examined an X-linked gene not involved in immune function, *ATRX*, which is known to undergo XCI in female cells (23, 26, 46). We found that *ATRX* is expressed in lymphocytes, and is predominantly monoallelic in naïve (99%) and activated (95%) female T cells, yet we also detected some biallelic-expressing cells (5%) present in activated T cells (Fig. 3C). Male cells only contained monoallelic-expressing cells for *ATRX* (100%) (Fig. S5*A*), similar to other X-linked genes examined. We conclude that the euchromatic nature of the Xi in female lymphocytes predisposes X-linked genes to become reactivated and biallelically expressed.

Next, we investigated how the euchromatic-like features of the Xi correlate with X-linked gene expression chromosome-wide in lymphocytes. We tested the hypothesis that if there is partial reactivation from the Xi in female lymphocytes, we would expect that healthy female cells, with an Xa and Xi, would have higher expression of X-linked genes compared with healthy male cells containing one Xa. We used gene set enrichment analysis (GSEA) to query sex-specific differences in gene expression by using an unbiased approach, examining published microarray datasets from human male and female mature naïve B cells (GSE30153). We found that there are three regions on the X chromosome that are overexpressed in female B cells compared with male B cells: p11, p22, and q13 (Fig. 3*D*). Region chrX.q13, containing 21 genes, was the most significantly overexpressed genomic region in female B cells [normalized enrichment score (NES) = 2.25; false discovery rate (FDR) $q = 0.003$] compared with male cells (Fig. 3*D*). This region contains the *XIST* gene, exclusively expressed in females, and we observed the same sex-biased expression in B cells, serving as a positive control for our analysis (Fig. 3*D*). We identified a gene signature from chrX.q13 of overexpressed genes specific to female B cells, listed in Fig. 3*D*, that are enriched at the leading edge (red region of the *x* axis) of the enrichment score plot. Importantly, two of these genes, *ITM2A* and *CXCR3*, are immunity-related and *CXCR3* is associated with autoimmunity (28, 47). The p arm of the X chromosome has more genes known to escape XCI compared with the q arm, explaining why genes from these two regions are expressed at higher levels in females compared with males. A number of genes known to escape XCI, including *EIF1AX*, *EIF2S3*, *OFD1*, and *ZFX* (23), are located within chrX.p22 and are enriched in female B cells. We found that the immunity-related genes *IL3FA* and *FOXP3*, located within regions chrX.p22 and chrX.p11, are overexpressed in female cells and are enriched at the leading edge of the enrichment score plots for female B cells. There is no evidence to date that *IL3FA* and *FOXP3* escape XCI in humans (23, 26). To test for the significance of immunity-related genes in sex-specific cell comparisons, we repeated the unbiased GSEA by using human fetal lung fibroblasts. We found that chrX.q13 was the most differentially expressed region in lung fibroblasts (NES = 1.52; FDR $q = 0.05$) similar to GSEA results using human B cells (Fig. S5*C*). As expected, *XIST* was the most differentially expressed gene that distinguishes male and female lung fibroblasts (fold change = 127). However, the other significantly enriched genes (*ATP7A, P2RY4, FOXO4, SLC16A2*) are not immunity-related and are known to escape from XCI (23, 26). We conclude that human female B cells contain regions along the X that are expressed at higher levels compared with male cells, and these regions contain immunity-related genes. These results are consistent with the euchromatic nature of the Xi in mammalian lymphocytes that could facilitate higher expression in lymphocytes.

YY1 and hnRNPU Proteins Localize XIST/Xist RNA Transcripts to the Xi in Activated T and B Cells from Humans and Mice. Naïve T and B cells express abundant levels of XIST/Xist RNA, but these transcripts do not associate with the Xi until these cells become activated. Therefore, we searched for candidate proteins known to bind XIST RNA that could function to recruit XIST RNA back to the Xi after lymphocyte stimulation. The nuclear scaffold protein SAF-A/hnRNPU is enriched on the Xi and is required for localizing Xist RNA to the Xi in embryonic stem cells during the initiation of XCI (48, 49). The transcription factor YY1 also tethers Xist RNA to the X during the initiation and maintenance stages of XCI, and activates *Xist/XIST* transcription (50, 51). Importantly, knockdown of hnRNPU or YY1 disrupts Xist RNA localization in post-XCI fibroblasts, resulting in a scattered pinpoint pattern similar to types II and III in lymphocytes. We found that YY1 and hnRNPU RNA and protein are expressed in naïve human female T cells, and that in vitro activation doubled transcriptional expression (Fig. S6*A*) and increased protein levels (Fig. S6*B*). Using siRNAs specific for YY1 or hnRNPU, we disrupted expression of these proteins in human mature naïve T cells, then stimulated the cells for 2–3 d. We verified knockdown efficiency for YY1 and hnRNPU in naïve and activated T cells by using qPCR and immunofluorescence (Fig. S6*D*). We found that hnRNPU or YY1 knockdown significantly reduced the number of canonical type I XIST RNA clouds from 25 to 10% (YY1 KD; $P = 0.02$) and 3% (hnRNPU KD; $P = 0.03$) (Fig. 4*B*). The percentage of activated human T cells with a type III XIST pattern increased from 30 to 47% (YY1 KD; $P = 0.03$) and 45% (hnRNPU KD; $P = 0.08$) (Fig. 4*B*), similar to what is observed when these proteins are disrupted in differentiating female mouse embryonic stem cells or embryonic fibroblasts (49, 50). Reduction of YY1 or hnRNPU in naïve or activated T cells did not affect XIST RNA transcript levels (Fig. S7*B*), further supporting a role for these proteins in localizing XIST RNA to the Xi rather than affecting *XIST* transcription.

In complementary experiments, we asked whether YY1 deletion would affect Xist RNA localization to the Xi in activated B cells from mice. Similar to human T cells, YY1 levels increased upon activation in female mouse B cells (Fig. S6*C*). We isolated mature naïve B cells from mice containing loxP sites flanking exon 1 of YY1 (9, 52), then deleted YY1 by introducing TAT-Cre (53) and then stimulated with lipopolysaccharide treatment (Fig. 4*D*). This method eliminates 85–100% of YY1 expression (Fig. S6*C*) (9), depending on the efficiency of the TAT-Cre transfection into B cells, and is more effective at reducing YY1 levels than siRNAs. YY1 depletion significantly reduced type I RNA clouds from 43 to 0–5% ($P = 0.004$) in replicate experiments. As expected, type III Xist patterns increased with YY1 deletion from 11 to 65% (Fig. 4 *E* and *F*). In conclusion, the known Xist RNA binding proteins YY1 and hnRNPU also function in activated lymphocytes to recruit XIST RNA back to the Xi in activated T and B cells.

SLE Patient B Cells Have Altered Distributions of XIST RNA Localization Patterns and Biallelic Expression of Immunity-Related X-Linked Genes. We next tested whether XIST RNA association to the Xi is further perturbed in SLE-derived lymphocytes. Using RNA FISH, we determined the percentage for each XIST RNA localization pattern (types I–IV) in immortalized B-cell lines derived from pediatric SLE patients and age-matched healthy controls (Fig. 5*A*). We did not observe a significant difference with the canonical type I XIST RNA clouds between SLE and control samples. However, SLE B cells had more type II patterns of XIST RNA localization

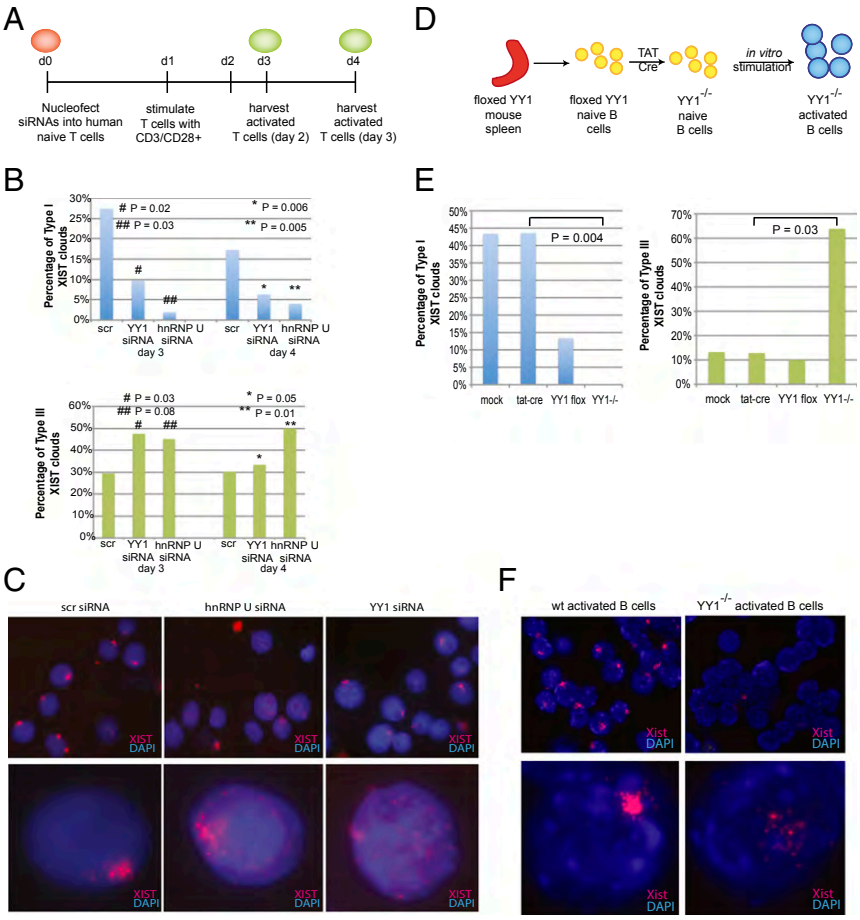

Fig. 4. YY1 and hnRNPU localize XIST/Xist RNA to the Xi in stimulated lymphocytes. (*A*) Experimental design for the knockdown experiments using human T cells. (*B*) Average percentages (for five experiments) quantifying type I and III XIST RNA patterns after YY1 or hnRNPU knockdown. Statistical significance calculated using Student's *t* test. (*C*) Representative XIST RNA images for activated T cells treated with scrambled siRNA (scr), siRNAs against hnRNPU, and siRNAs against YY1. Nuclear distribution of XIST RNA transcripts for each condition are shown below. (*D*) Experimental design for YY1 deletion in mouse B cells. (*E*) Quantification of type I and type III Xist RNA patterns in wild-type and YY1$^{-/-}$ activated B cells. Statistical significance calculated for averages from two independent experiments using Student's *t* test. (*F*) Representative Xist RNA images for wild-type and YY1$^{-/-}$ activated B cells.

relative to controls (P = 0.04). The most significant difference between SLE and control B cells was with the type III pattern, where 50% of the control cells were type III and SLE B cells had 10–30% type III cells (P = 0.006). We found that SLE B cells had more cells missing XIST RNA transcript accumulation within the nucleus (the type IV pattern) compared with normal B cells (P = 0.05). SLE B cells also had more type II patterns of XIST RNA localization relative to controls (P = 0.04). XIST RNA transcript levels were similar between normal and SLE B-cell lines (Fig. S7*A*), indicating that XIST RNA is not limiting in SLE cells. We also examined the levels of YY1 and hnRNPU transcripts and proteins in SLE B cells, and found similar expression for SLE and control lines (Fig. S8 *B* and *C*). Thus, XIST RNA exhibits abnormal localization patterns in SLE B cells, suggesting that X-silencing mechanisms may be different in SLE.

Next, we investigated whether these differences with XIST RNA localization were correlated with differences with allelic expression of X-linked immunity-related genes. We used RNA FISH to examine nascent transcription of three X-linked immunity-related genes typically overexpressed in lymphocytes from SLE patients: *CD40LG, CXCR3,* and *TRL7*. We determined the number of cells with either monoallelic (one pinpoint) or biallelic expression (two pinpoints), using immortalized B-cell lines generated from pediatric SLE patients or healthy female age-matched samples. We found that normal B-cell lines had mostly monoallelic expression of *CD40LG* (36–47% of cells), yet we also detected some biallelic-expressing B cells (4–20%; Fig. 5*B*), similar to our observations in activated T cells (Fig. 3*C*). *CD40LG* is normally overexpressed in SLE patient T cells, but is also ectopically expressed in SLE patient B cells (54). B-cell lines from three different pediatric SLE patients had slightly more biallelic-expressing SLE B cells for *CD40LG* (17–33%; P = 0.09) compared with healthy control lines (Fig. 5*B*). We found that SLE B-cell lines also had fewer cells with monoallelic expression of *CD40LG* (22–29%; P = 0.002) compared with healthy controls. Consistent with a trend toward more biallelic cells, SLE B cells also expressed more *CD40LG* transcripts compared with healthy controls (P = 0.033). In contrast to *CD40LG*, we saw no difference for monoallelic and biallelic expression of *CXCR3* (Fig. 5*B*). We also examined the expression of *TRL7*, which is overexpressed in SLE patient B cells (55). We detected similar levels of biallelic expression of *TLR7* in both normal (12–14%) and SLE B cells (9–23%), yet SLE lines had more TLR7 transcripts than normal lines (Fig. 5 *B* and *C*; P = 5.6e−6). In conclusion, biallelic expression of X-linked immunity-related genes was observed in both normal and SLE patient B cells, and the increased expression from the Xi could result from atypical XIST RNA localization patterns.

Lastly, we investigated whether altered distributions of XIST RNA patterns in SLE patients could reflect expression differences with X-linked genes. Because we found that a chrX.q13 gene signature distinguished male and female B cells (Fig. 3*D*), we examined whether this region is overexpressed in female SLE patients compared with healthy female controls. We used GSEA to query which regions of the X chromosome were overexpressed in female SLE B cells compared with healthy female B cells (GSE30153). As expected, we found that chrX.q13 had the greatest enrichment of overexpressed X-linked genes in SLE female B-cell samples (Fig. 5*D*). Six genes within this region, *KIF4A, OGT, HMGN5, NONO, CXCR3,* and *ITM2A*, were significantly enriched at the leading edge (red area of x axis) for the enrichment score plot (Fig. S8*A*). Importantly, both *OGT* and *CXCR3* are overexpressed in female SLE patient lymphocytes (28), consistent with our results. Our findings suggest the intriguing hypothesis that altered XIST RNA localization to the Xi

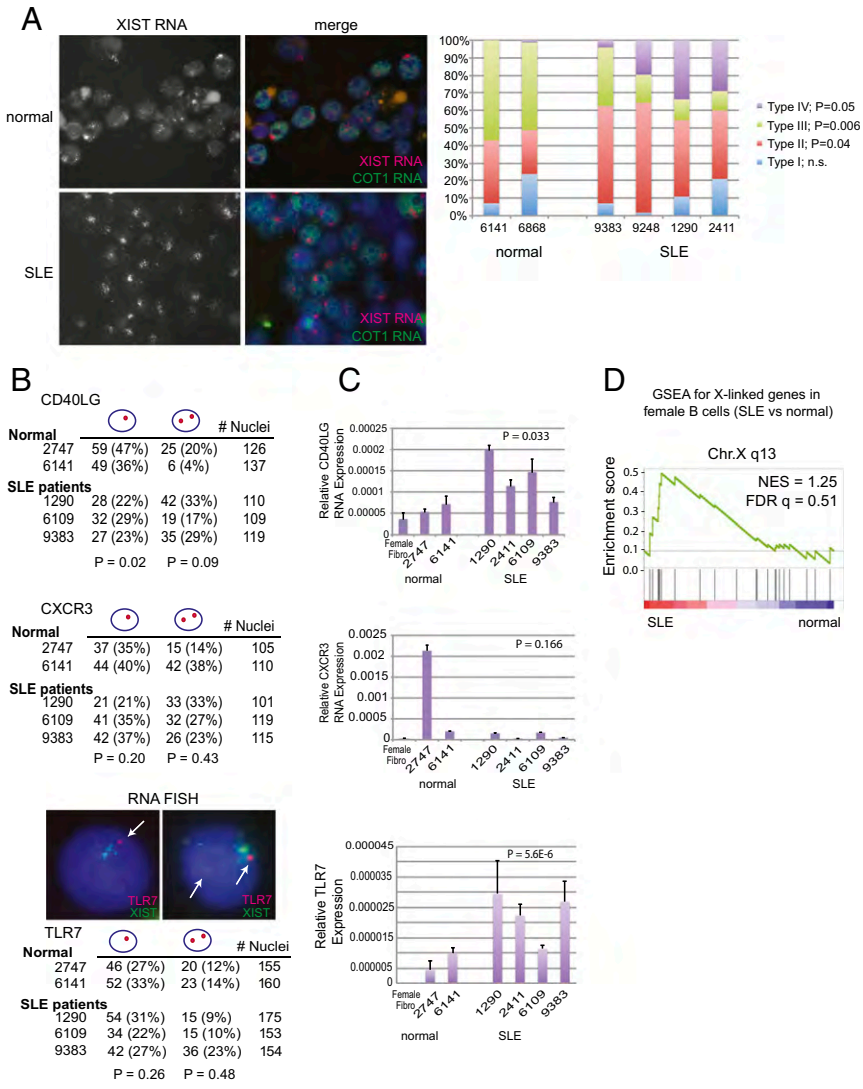

Fig. 5. SLE patient B cells have different XIST RNA patterns and greater biallelic expression of immunity-related X-linked genes. (*A*) XIST (red) and COT1 (green) RNA FISH field images for immortalized B-cell lines from a pediatric SLE patient and a healthy age-matched control. Quantification of XIST RNA localization patterns for SLE B-cell lines and healthy controls. (*B*) RNA FISH analyses at single-cell resolution for allele-specific expression of *CD40LG*, *CXCR3*, and *TRL7* in SLE patient and healthy control B-cell lines. (*C*) qRT-PCR analysis of *CD40LG*, *CXCR3*, and *TRL7* in SLE and normal B-cell lines. *P* values were calculated by using Student's *t* test. (*D*) GSEA comparing gene expression differences from the X (chrX.q13) in human female SLE naïve B cells (during inactive disease; 15 samples) to healthy female B cells (7 samples).

promotes higher expression of immunity-related X-linked genes from chrX.q13.

Discussion

Here, we have demonstrated that female lymphocytes in humans and mice do not maintain XCI with the same fidelity as other somatic cells. Specifically, whereas XIST/Xist RNA is thought to remain localized to the Xi in all somatic cells, mature naïve lymphocytes lack XIST/Xist RNA clouds. This study is the first, to our knowledge, to classify differences with XIST/Xist RNA localization patterns in lymphocytes. The molecular mechanisms responsible for these four types of XIST RNA patterns, and the significance of type II and III cells, are unknown at this time and warrant further investigation. Also unclear is how these XIST/Xist RNA patterns correlate with SLE disease severity, and whether other autoimmune disorders involving T and B cells also exhibit different localization. Moreover, we found that the Xi in naïve lymphocytes lacks enrichment of H3K27me3, H4K20me1/3, H2AUb, and macroH2A, all hallmarks of heterochromatin. The absence of these modifications is consistent with observed increased expression of immunity-related X-linked genes in human naïve B cells, and the presence of some T cells with biallelic expression of *CXCR3*. These euchromatic features of the lymphocyte Xi are in agreement with a recent study profiling the open regions of chromatin by using the Assay of Transposase Accessible Chromatin (ATAC) Seq comparing female and male $CD4^+$ T cells (27). Qu et al. also found that females have more accessible elements on the X compared with male cells. Our study also observed that some activated T (Fig. 3*C*) and B cells (Fig. 5*B*) have biallelic expression of X-linked immunity-related genes. We conclude that this unusual maintenance of XCI in naïve and activated lymphocytes predisposes portions of the Xi to become reactivated and increase expression of X-linked genes, providing a potential mechanistic explanation for why female mammals and individuals with multiple X's are more susceptible to autoimmunity.

The biological reason for XIST/Xist RNA localization changes in female lymphocytes is unknown. One possibility is that female mammals have evolved this mechanism to relax Xi silencing to increase the expression of immunity-related genes that may be beneficial for fighting infection. Lymphocyte gene expression from the Xi could be caused by escape from XCI or gene reactivation. Although 10% of human X-linked genes exhibit variable escape among individuals and in tissues (23, 26), it is unlikely that X-linked autoimmunity-related genes are escaping X silencing in lymphocytes. Escape from XCI has been profiled in human fibroblasts and peripheral blood mononuclear cells, and *CD40LG* and *CXCR3* were not expressed from the Xi in any of these cell types (26). Our observations of T cells with biallelic expression suggests that the origin is likely due to gene-specific reactivation in a subpopulation of female lymphocytes, which results in increased expression. We speculate that

immunity-related genes such as *CD40LG* and *CXCR3* might be more susceptible to reactivation from the Xi in lymphocytes because of the euchromatic chromatin of the Xi. Another possibility is that immunity-related genes on chrX.q13, the region containing the *XIST* gene, can become reactivated and expressed from the Xi because XIST RNA is not localized to the Xi in naïve lymphocytes (Fig. 1). Support for this hypothesis is the observation that human female pluripotent stem cells lacking XIST RNA reactivate regions of the Xi and overexpress X-linked genes (56, 57).

Whereas the majority of naive human and mouse peripheral T cells lacked XIST/Xist RNA association with the Xi, a minority (~1–5%) contained type I XIST RNA clouds. These few cells could either represent a specific subset of T cells where XIST remains localized to the Xi, or alternatively could represent circulating antigen-stimulated T cells. Our data contrasts with a previous study by Savarese et al. in which the absence of Xist RNA clouds and H3K27me3 was noted in immature lymphocytes, but Xist RNA clouds were observed in ~50% in mature T and B cells (31). This discrepancy could be due to activation of an immune response in the animals from the Savarese et al. study before cell isolation. Savarese et al. also examined whether genes on the Xi were reactivated in immature lymphocytes by using F_1 hybrid mice carrying an *Xist* deletion on the maternal allele, where reactivated genes would be expressed from the paternal allele. The authors examined four X-linked genes, *Xist*, *G6pd*, *Pctk1*, and *Pgk1*, and did not observe any expression from the paternal X by using allele-specific RT-PCR. However, this study did not examine the expression of X-linked immunity-related genes in lymphocytes from these F_1 hybrid animals, which may be expressed at higher levels.

Recent work has identified new Xist RNA binding proteins that function in the initiation or maintenance of XCI in mice (58–60). YY1 and hnRNPU are known Xist RNA binding proteins that localize the RNA to the Xi during the initiation of XCI (YY1) and maintenance phase (hnRNPU) (49, 50). YY1 can also recruit a variety of proteins to DNA, most notably polycomb repressive complex 1 (PRC1) and PRC2 (61–63). Importantly, these complexes are involved in initiating XCI during early development (43, 64–66). Our studies have identified a previously unidentified localization function for these proteins: the return of XIST/Xist RNA to the Xi during the transition from quiescence to activation in female lymphocytes. The YY1 knockout and knockdown studies indicate that this protein is required for the early stages of Xist/XIST cloud formation during lymphocyte activation, suggesting that XIST RNA return to the Xi precedes PRC2 deposition of H3K27me3. Importantly, these observations provide a testable model system to investigate the mechanisms of Xist/XIST RNA cloud formation in both mouse and human lymphocytes. Naïve lymphocytes express low levels of YY1 and hnRNPU, which may explain why the XIST/Xist RNA transcript does not remain associated with the Xi in these cells. Activated lymphocytes contain greater amounts of these proteins, probably due to genome-wide transcriptional activation that occurs together with increased cell proliferation as naïve lymphocytes exit quiescence. Additional experiments are necessary to determine how the nuclear organization context (quiescent versus activated) and the concentration of Xist binding proteins influences Xist RNA recruitment back to the Xi. With the recent findings that Xist RNA physically interacts with 80–250 proteins (60), it is likely that additional proteins will be required to localize XIST/Xist back to the Xi.

The only human female cells previously shown to lack XIST RNA clouds are a predominant subset (class III) of female pluripotent stem cells (hPSCs) with an "eroded" Xi (56, 57, 67). Female hPSCs are epigenetically unstable for XCI, and these cells will irreversibly silence the *XIST* gene during routine culture. Class III hPSCs also lack cytologically visible enrichment of H3K27me3, H4K20me, macroH2A, and H2A-ub on the Xi (46, 68, 69), resulting in a partially reactivated Xi. These cells overexpress a variable set of X-linked genes (56, 57), indicating that loss of XIST RNA doesn't always reactivate the same genes or regions in hPSCs. However, gene reactivation from the Xi in the absence of XIST/Xist RNA may be more uniform in human and mouse lymphocytes. Deletion of *Xist* in the hematopoietic cell lineage partially reactivates the Xi, resulting in increased expression of ~86 X-linked genes in blood cells, some which are involved in hematopoiesis and cell cycle regulation (70). Interestingly, this list includes two immunity genes *CXCR3* and *TRL7* whose overexpression is associated with lupus (71–73), which suggests that immunity-related genes are somehow poised for reactivation in the blood lineage when Xist RNA is missing. Future work is required to determine the specificity of X-linked gene reactivation when *Xist* is deleted, and how partial reactivation of Xi changes depending on the cell type.

Materials and Methods

Mammalian Cell Isolation and Lines. Human naïve lymphocytes (all deidentified) were collected by the University of Pennsylvania Pathology BioResouce Human Immunology Core facility. Immortalized B-cell lines [generated by infection with Epstein–Barr virus (EBV)] from five pediatric SLE patients and three healthy females (all deidentified) were derived by Hakon Hakonerson's group at the Children's Hospital of Philadelphia and approved by the Children's Hospital of Philadelphia Institutional Review Board (IRB). Patients and their families were recruited through the Children's Hospital of Philadelphia clinic or CHOP outreach clinics. Written informed consent was obtained from the participants or their parents by using IRB-approved consent forms before enrollment in the project. In vitro activation of lymphocytes is described in *SI Materials and Methods*. Animal experiments were approved by the University of Pennsylvania Institutional Animal Care and Use Committee.

RNA FISH, DNA FISH, and Immunofluorescence. RNA and DNA FISH were carried out as described (56, 67, 74). Human XIST probe (exon 1) and mouse Xist probe (Sx9) were labeled by nick translation with Cy3-dUTP, and COT-1 DNA was labeled with fluoroscein-12-dUTP. Three oligo probes (20 nt in length) specific for XIST were designed to recognize regions within exon 1, and labeled with one Cy3 molecule at the 5′ end (IDT). StarFISH X chromosome paints (Cambio) for DNA FISH were hybridized per manufacturer's instructions.

ACKNOWLEDGMENTS. We thank J. Pearson, J. Wang, M. Bartolomei, K. Sarma, and L. King for reading this manuscript and critical discussions; the various laboratories across the University of Pennsylvania campus that shared mouse lymphocytes: S. Fuchs, A. Hu, C. Hunter, and J. Wherry; J. Riley and A. Medvec for instruction with human T-cell activation; D. Beiting for help with bioinformatic analysis; C. Berry for assistance with statistical analyses; all human blood donors recruited by the University of Pennsylvania; and J. Rinn and E. Hacisuleyman for assistance with hnRNPU siRNAs and knockdown. Human XIST oligo probes were designed by B. Del Rosario. The hnRNPU monoclonal antibody was a generous gift from G. Dreyfuss. EBV-immortalized patient B cells were collected by the Children's Hospital of Philadelphia patient repository supervised by H. Hakonerson. This work was supported by the McCabe research foundation (M.C.A.), a grant with the Pennsylvania Department of Health (to M.C.A.), the Lupus Foundation (C.M.S. and M.C.A.), and NIH Grant T32 GM-07229 (to C.M.S.).

1. Ross MT, et al. (2005) The DNA sequence of the human X chromosome. *Nature* 434(7031):325–337.
2. Migeon BR (2006) The role of X inactivation and cellular mosaicism in women's health and sex-specific diseases. *JAMA* 295(12):1428–1433.
3. Spolarics Z (2007) The X-files of inflammation: Cellular mosaicism of X-linked polymorphic genes and the female advantage in the host response to injury and infection. *Shock* 27(6):597–604.
4. Butterworth M, McClellan B, Allansmith M (1967) Influence of sex in immunoglobulin levels. *Nature* 214(5094):1224–1225.
5. Purtilo DT, Sullivan JL (1979) Immunological bases for superior survival of females. *Am J Dis Child* 133(12):1251–1253.
6. Thompson DJ, Gezon HM, Rogers KD, Yee RB, Hatch TF (1966) Excess risk of staphylococcal infection and disease in newborn males. *Am J Epidemiol* 84(2):314–328.
7. Green MS (1992) The male predominance in the incidence of infectious diseases in children: A postulated explanation for disparities in the literature. *Int J Epidemiol* 21(2):381–386.
8. Libert C, Dejager L, Pinheiro I (2010) The X chromosome in immune functions: When a chromosome makes the difference. *Nat Rev Immunol* 10(8):594–604.
9. Selmi C, Brunetta E, Raimondo MG, Meroni PL (2012) The X chromosome and the sex ratio of autoimmunity. *Autoimmun Rev* 11(6-7):A531–A537.
10. Cooney CM, et al. (2009) 46,X,del(X)(q13) Turner's syndrome women with systemic lupus erythematosus in a pedigree multiplex for SLE. *Genes Immun* 10(5):478–481.

11. Scofield RH, et al. (2008) Klinefelter's syndrome (47,XXY) in male systemic lupus erythematosus patients: Support for the notion of a gene-dose effect from the X chromosome. *Arthritis Rheum* 58(8):2511–2517.
12. Lyon MF (1961) Gene action in the X-chromosome of the mouse (Mus musculus L.). *Nature* 190:372–373.
13. Payer B, Lee JT (2008) X chromosome dosage compensation: How mammals keep the balance. *Annu Rev Genet* 42:733–772.
14. Brown CJ, et al. (1991) A gene from the region of the human X inactivation centre is expressed exclusively from the inactive X chromosome. *Nature* 349(6304):38–44.
15. Brockdorff N, et al. (1991) Conservation of position and exclusive expression of mouse Xist from the inactive X chromosome. *Nature* 351(6324):329–331.
16. Jonkers I, et al. (2008) Xist RNA is confined to the nuclear territory of the silenced X chromosome throughout the cell cycle. *Mol Cell Biol* 28(18):5583–5594.
17. Plath K, et al. (2003) Role of histone H3 lysine 27 methylation in X inactivation. *Science* 300(5616):131–135.
18. Mermoud JE, Popova B, Peters AH, Jenuwein T, Brockdorff N (2002) Histone H3 lysine 9 methylation occurs rapidly at the onset of random X chromosome inactivation. *Curr Biol* 12(3):247–251.
19. Csankovszki G, Panning B, Bates B, Pehrson JR, Jaenisch R (1999) Conditional deletion of Xist disrupts histone macroH2A localization but not maintenance of X inactivation. *Nat Genet* 22(4):323–324.
20. Kohlmaier A, et al. (2004) A chromosomal memory triggered by Xist regulates histone methylation in X inactivation. *PLoS Biol* 2(7):E171.
21. Smith KP, Byron M, Clemson CM, Lawrence JB (2004) Ubiquitinated proteins including uH2A on the human and mouse inactive X chromosome: Enrichment in gene rich bands. *Chromosoma* 113(6):324–335.
22. Peeters SB, Cotton AM, Brown CJ (2014) Variable escape from X-chromosome inactivation: Identifying factors that tip the scales towards expression. *BioEssays* 36(8):746–756.
23. Carrel L, Willard HF (2005) X-inactivation profile reveals extensive variability in X-linked gene expression in females. *Nature* 434(7031):400–404.
24. Yang F, Babak T, Shendure J, Disteche CM (2010) Global survey of escape from X inactivation by RNA-sequencing in mouse. *Genome Res* 20(5):614–622.
25. Carrel L, Willard HF (1999) Heterogeneous gene expression from the inactive X chromosome: An X-linked gene that escapes X inactivation in some human cell lines but is inactivated in others. *Proc Natl Acad Sci USA* 96(13):7364–7369.
26. Cotton AM, et al. (2011) Chromosome-wide DNA methylation analysis predicts human tissue-specific X inactivation. *Hum Genet* 130(2):187–201.
27. Qu K, et al. (2015) Individuality and variation of personal regulomes in primary human T cells. *Cell Syst* 1(1):51–61.
28. Hewagama A, et al.; Michigan Lupus Cohort (2013) Overexpression of X-linked genes in T cells from women with lupus. *J Autoimmun* 41:60–71.
29. Lu Q, et al. (2007) Demethylation of CD40LG on the inactive X in T cells from women with lupus. *J Immunol* 179(9):6352–6358.
30. Brown CJ, et al. (1992) The human XIST gene: Analysis of a 17 kb inactive X-specific RNA that contains conserved repeats and is highly localized within the nucleus. *Cell* 71(3):527–542.
31. Savarese F, Flahndorfer K, Jaenisch R, Busslinger M, Wutz A (2006) Hematopoietic precursor cells transiently reestablish permissiveness for X inactivation. *Mol Cell Biol* 26(19):7167–7177.
32. Hall LL, et al. (2002) An ectopic human XIST gene can induce chromosome inactivation in postdifferentiation human HT-1080 cells. *Proc Natl Acad Sci USA* 99(13):8677–8682.
33. Clemson CM, Hall LL, Byron M, McNeil J, Lawrence JB (2006) The X chromosome is organized into a gene-rich outer rim and an internal core containing silenced nongenic sequences. *Proc Natl Acad Sci USA* 103(20):7688–7693.
34. Namekawa SH, Payer B, Huynh KD, Jaenisch R, Lee JT (2010) Two-step imprinted X inactivation: Repeat versus genic silencing in the mouse. *Mol Cell Biol* 30(13): 3187–3205.
35. Andersson J, Sjöberg O, Möller G (1972) Induction of immunoglobulin and antibody synthesis in vitro by lipopolysaccharides. *Eur J Immunol* 2(4):349–353.
36. Krieg AM, et al. (1995) CpG motifs in bacterial DNA trigger direct B-cell activation. *Nature* 374(6522):546–549.
37. Ledderose C, Heyn J, Limbeck E, Kreth S (2011) Selection of reliable reference genes for quantitative real-time PCR in human T cells and neutrophils. *BMC Res Notes* 4:427.
38. Wutz A, Jaenisch R (2000) A shift from reversible to irreversible X inactivation is triggered during ES cell differentiation. *Mol Cell* 5(4):695–705.
39. Sarma K, Levasseur P, Aristarkhov A, Lee JT (2010) Locked nucleic acids (LNAs) reveal sequence requirements and kinetics of Xist RNA localization to the X chromosome. *Proc Natl Acad Sci USA* 107(51):22196–22201.
40. Beletskii A, Hong YK, Pehrson J, Egholm M, Strauss WM (2001) PNA interference mapping demonstrates functional domains in the noncoding RNA Xist. *Proc Natl Acad Sci USA* 98(16):9215–9220.
41. Grigoryev SA, Nikitina T, Pehrson JR, Singh PB, Woodcock CL (2004) Dynamic relocation of epigenetic chromatin markers reveals an active role of constitutive heterochromatin in the transition from proliferation to quiescence. *J Cell Sci* 117(Pt 25): 6153–6162.
42. Costanzi C, Stein P, Worrad DM, Schultz RM, Pehrson JR (2000) Histone macroH2A1 is concentrated in the inactive X chromosome of female preimplantation mouse embryos. *Development* 127(11):2283–2289.
43. de Napoles M, et al. (2004) Polycomb group proteins Ring1A/B link ubiquitylation of histone H2A to heritable gene silencing and X inactivation. *Dev Cell* 7(5):663–676.
44. Changolkar LN, Pehrson JR (2006) macroH2A1 histone variants are depleted on active genes but concentrated on the inactive X chromosome. *Mol Cell Biol* 26(12):4410–4420.
45. Smetana K, Karhan J, Trneny M (2011) Heterochromatin condensation in central and peripheral nuclear regions of maturing lymphocytes in the peripheral blood of patients suffering from B chronic lymphocytic leukemia - a cytochemical study. *Neoplasma* 58(6):476–481.
46. Tchieu J, et al. (2010) Female human iPSCs retain an inactive X chromosome. *Cell Stem Cell* 7(3):329–342.
47. Enghard P, et al. (2009) CXCR3+CD4+ T cells are enriched in inflamed kidneys and urine and provide a new biomarker for acute nephritis flares in systemic lupus erythematosus patients. *Arthritis Rheum* 60(1):199–206.
48. Helbig R, Fackelmayer FO (2003) Scaffold attachment factor A (SAF-A) is concentrated in inactive X chromosome territories through its RGG domain. *Chromosoma* 112(4):173–182.
49. Hasegawa Y, et al. (2010) The matrix protein hnRNP U is required for chromosomal localization of Xist RNA. *Dev Cell* 19(3):469–476.
50. Jeon Y, Lee JT (2011) YY1 tethers Xist RNA to the inactive X nucleation center. *Cell* 146(1):119–133.
51. Makhlouf M, et al. (2014) A prominent and conserved role for YY1 in Xist transcriptional activation. *Nat Commun* 5:4878.
52. Affar B, et al. (2006) Essential dosage-dependent functions of the transcription factor yin yang 1 in late embryonic development and cell cycle progression. *Mol Cell Biol* 26(9):3565–3581.
53. Joshi SK, Hashimoto K, Koni PA (2002) Induced DNA recombination by Cre recombinase protein transduction. *Genesis* 33(1):48–54.
54. Desai-Mehta A, Lu L, Ramsey-Goldman R, Datta SK (1996) Hyperexpression of CD40 ligand by B and T cells in human lupus and its role in pathogenic autoantibody production. *J Clin Invest* 97(9):2063–2073.
55. García-Ortiz H, et al. (2010) Association of TLR7 copy number variation with susceptibility to childhood-onset systemic lupus erythematosus in Mexican population. *Ann Rheum Dis* 69(10):1861–1865.
56. Anguera MC, et al. (2012) Molecular signatures of human induced pluripotent stem cells highlight sex differences and cancer genes. *Cell Stem Cell* 11(1):75–90.
57. Mekhoubad S, et al. (2012) Erosion of dosage compensation impacts human iPSC disease modeling. *Cell Stem Cell* 10(5):595–609.
58. Chu C, et al. (2015) Systematic discovery of Xist RNA binding proteins. *Cell* 161(2): 404–416.
59. McHugh CA, et al. (2015) The Xist lncRNA interacts directly with SHARP to silence transcription through HDAC3. *Nature* 521(7551):232–236.
60. Minajigi A, et al. (2015) Chromosomes. A comprehensive Xist interactome reveals cohesin repulsion and an RNA-directed chromosome conformation. *Science* 349(6245):aab2276.
61. Sawada S, Scarborough JD, Killeen N, Littman DR (1994) A lineage-specific transcriptional silencer regulates CD4 gene expression during T lymphocyte development. *Cell* 77(6):917–929.
62. Wilkinson FH, Park K, Atchison ML (2006) Polycomb recruitment to DNA in vivo by the YY1 REPO domain. *Proc Natl Acad Sci USA* 103(51):19296–19301.
63. Atchison L, Ghias A, Wilkinson F, Bonini N, Atchison ML (2003) Transcription factor YY1 functions as a PcG protein in vivo. *EMBO J* 22(6):1347–1358.
64. Zhao J, Sun BK, Erwin JA, Song JJ, Lee JT (2008) Polycomb proteins targeted by a short repeat RNA to the mouse X chromosome. *Science* 322(5902):750–756.
65. Kalantry S, et al. (2006) The Polycomb group protein Eed protects the inactive X-chromosome from differentiation-induced reactivation. *Nat Cell Biol* 8(2):195–202.
66. Schoeftner S, et al. (2006) Recruitment of PRC1 function at the initiation of X inactivation independent of PRC2 and silencing. *EMBO J* 25(13):3110–3122.
67. Silva SS, Rowntree RK, Mekhoubad S, Lee JT (2008) X-chromosome inactivation and epigenetic fluidity in human embryonic stem cells. *Proc Natl Acad Sci USA* 105(12):4820–4825.
68. Shen Y, et al. (2008) X-inactivation in female human embryonic stem cells is in a nonrandom pattern and prone to epigenetic alterations. *Proc Natl Acad Sci USA* 105(12):4709–4714.
69. Hall LL, et al. (2008) X-inactivation reveals epigenetic anomalies in most hESC but identifies sublines that initiate as expected. *J Cell Physiol* 216(2):445–452.
70. Yildirim E, et al. (2013) Xist RNA is a potent suppressor of hematologic cancer in mice. *Cell* 152(4):727–742.
71. Hwang SH, et al. (2012) B cell TLR7 expression drives anti-RNA autoantibody production and exacerbates disease in systemic lupus erythematosus-prone mice. *J Immunol* 189(12):5786–5796.
72. Pisitkun P, et al. (2006) Autoreactive B cell responses to RNA-related antigens due to TLR7 gene duplication. *Science* 312(5780):1669–1672.
73. Moser K, et al. (2012) CXCR3 promotes the production of IgG1 autoantibodies but is not essential for the development of lupus nephritis in NZB/NZW mice. *Arthritis Rheum* 64(4):1237–1246.
74. Erwin JA, Lee JT (2010) Characterization of X-chromosome inactivation status in human pluripotent stem cells. *Curr Protoc Stem Cell Biol*, Chapter 1, Unit 1B 6.
75. Yung RL, Quddus J, Chrisp CE, Johnson KJ, Richardson BC (1995) Mechanism of drug-induced lupus. I. Cloned Th2 cells modified with DNA methylation inhibitors in vitro cause autoimmunity in vivo. *J Immunol* 154:3025–3035.
76. Subramanian S (2006) A *Tlr7* translocation accelerates systemic autoimmunity in murine lupus. *Proc Natl Acad Sci USA* 103(26):9970–9975.
77. Garaud JC, et al. (2011) B cell signature during inactive systemic lupus is heterogeneous: Toward a biological dissection of lupus. *PLoS One* 6(8):e23900.
78. Peng R, et al. (2013) Bleomycin induces molecular changes directly relevant to idiopathic pulmonary fibrosis: A model for "active" disease. *PLoS One* 8(4):e59348.
79. Subramanian A, et al. (2005) Gene set enrichment analysis: A knowledge-based approach for interpreting genome-wide expression profiles. *Proc Natl Acad Sci USA* 102(43):15545–15550.